

## Supplementary information

### Electrochemically induced CO<sub>2</sub> capture enabled by aqueous quinone flow chemistry

Yan Jing,<sup>1,2,3</sup> Kiana Amini,<sup>2,3</sup> Dawei Xi,<sup>2</sup> Shijian Jin,<sup>2</sup> Abdulrahman M. Alfaraidi,<sup>2</sup> Emily F. Kerr,<sup>1</sup> Roy G. Gordon,<sup>1,2\*</sup> Michael J. Aziz<sup>2\*</sup>

<sup>1</sup>. Department of Chemistry and Chemical Biology, Harvard University, Cambridge, Massachusetts 02138, United States

<sup>2</sup>. John A. Paulson School of Engineering and Applied Sciences, Harvard University, Cambridge, Massachusetts 02138, United States

<sup>3</sup>. These authors contributed equally to this work.

\* E-mail: [gordon@chemistry.harvard.edu](mailto:gordon@chemistry.harvard.edu); [maziz@harvard.edu](mailto:maziz@harvard.edu).

## Table of Contents

<b>General experimental procedures .....</b>	<b>2</b>
<b>Solubility of anthraquinones in different stages in different supporting salts.....</b>	<b>4</b>
Table S1   Solubility behavior of anthraquinones in different supporting salts.....	4
Figure S1   <sup>1</sup> H and <sup>13</sup> C NMR spectra of 0.1 M AQDS, AQDS <sup>2-</sup> , AQDS(CO <sub>2</sub> ) <sup>2-</sup> 1 M TMACl D <sub>2</sub> O solutions.....	4
<b>Compatibility issue between bulky alkylammonium cation (TBA<sup>+</sup>) and cation-exchange membrane.....</b>	<b>5</b>
Figure S2   Electrochemical impedance spectroscopy (EIS) measurement of 2,6-D2PEAQ flow cells. ....	5
Figure S3   Stacked <sup>1</sup> H NMR spectra of 1,8-BTMAPAQ in three states. ....	5
Figure S4   Electrochemical impedance spectroscopy (EIS) measurement of 0.1 M BTMAPAQ   0.1 M FeNCl flow cells.....	6
Figure S5   Voltage profiles and CO <sub>2</sub> partial pressure during the electrochemical reduction and oxidation of BTMAPAQs.....	6
<b>Chemical CO<sub>2</sub> capture, release, and sequestration procedure in the absence of O<sub>2</sub>.....</b>	<b>7</b>
Figure S6   Chemically induced CO <sub>2</sub> capture, release, and sequestration.....	7
<b>Electrochemical CO<sub>2</sub> capture in O<sub>2</sub>-free environment .....</b>	<b>8</b>
Figure S7   Cumulative CO <sub>2</sub> captured during the charge and rest time for the fourth cycle of Figure 4a 0.5 bar CO <sub>2</sub> experiment. ....	8
Figure S8   CO <sub>2</sub> capture and release cycling in a flow cell.....	8
Figure S9   CO <sub>2</sub> capture and release using different CO <sub>2</sub> partial pressure values in a flow cell .....	9
Figure S10   CO <sub>2</sub> capture and release cycling at different current densities (20, 40, 60, 80, 100 mA/cm <sup>2</sup> ) in inlet CO <sub>2</sub> partial pressure of 0.1 and 0.5 bar in a flow cell.....	9
Figure S11   CO <sub>2</sub> capture and release cycling at a current density of 20 mA/cm <sup>2</sup> in inlet CO <sub>2</sub> partial pressure of 0.5 bar in a flow cell.....	10
Figure S12   CO <sub>2</sub> capture and release cycling where the capture occurs in an inlet CO <sub>2</sub> partial pressure of 0.1 bar and the release occur in an inlet CO <sub>2</sub> partial pressure of 1 bar in a flow cell.....	11
Concentrated cell test.....	12
Figure S13   CO <sub>2</sub> partial pressure changes over the electrochemical reduction and oxidation cycling of 1,4- and 1,5-BTMAPAQs.....	12

Oxygen sensitivity of reduced anthraquinones.....	13
Figure S14   $^1\text{H}$ NMR tracking of chemically synthesized 0.1 M 2,6-D2PEAQ( $\text{CO}_2$ ) $^{2-}$ in 1 M TBABr D <sub>2</sub> O over days while air was gradually introduced. ....	13
Figure S15   $^1\text{H}$ NMR tracking of chemically synthesized 0.1 M 1,8-BTMAPAQ $^{2-}$ (a) and 0.1 M 1,8-BTMAPAQ( $\text{CO}_2$ ) $^{2-}$ (b) in 1 M TBABr D <sub>2</sub> O over days while air was gradually introduced.....	14
Figure S16   $^1\text{H}$ NMR tracking of chemically synthesized 0.1 M 1,5-BTMAPAQ $^{2-}$ (a) and 0.1 M 1,5-BTMAPAQ( $\text{CO}_2$ ) $^{2-}$ (b) in 1 M KCl D <sub>2</sub> O over days while air was gradually introduced. ....	14
Figure S17   $^1\text{H}$ NMR tracking of chemically synthesized 0.1 M 1,4-BTMAPAQ $^{2-}$ (a) and 0.1 M 1,4-BTMAPAQ( $\text{CO}_2$ ) $^{2-}$ (b) in 1 M KCl D <sub>2</sub> O over days while air was gradually introduced. ....	15
Figure S18   $^1\text{H}$ NMR tracking of chemically synthesized 0.1 M AQDS( $\text{CO}_2$ ) $^{2-}$ in 1 M TMACl D <sub>2</sub> O over days while air was gradually introduced. ....	15
Figure S19   $^1\text{H}$ NMR tracking of chemically synthesized 0.1 M AQ-1,8-3E-OH( $\text{CO}_2$ ) $^{2-}$ in 1 M TBABr D <sub>2</sub> O over days while air was gradually introduced. ....	16
Table S2   Coulombic efficiencies of BTMAPAQs   FcNCl flow cells while the BTMAPAQ electrolytes were kept in the atmosphere with different ratios of O <sub>2</sub> /CO <sub>2</sub> /N <sub>2</sub> . ....	16
<b>Chemical CO<sub>2</sub> capture, release, and sequestration procedure in the presence of O<sub>2</sub> .....</b>	<b>17</b>
Figure S20   Chemically induced CO <sub>2</sub> capture, release, and sequestration. ....	17
<b>Electrochemical CO<sub>2</sub> capture in the presence of O<sub>2</sub> .....</b>	<b>18</b>
Figure S21   Schematic of the electrochemical CO <sub>2</sub> setup in the presence of O <sub>2</sub> .....	18
Figure S22   Setup of electrochemical CO <sub>2</sub> capture with aqueous quinone flow chemistry.....	18
Figure S23   A close look of tube positioning in the anthraquinone electrolyte Falcon tube. ....	19
Figure S24   Variation of CO <sub>2</sub> and O <sub>2</sub> partial pressure during the electrochemical reduction and oxidation of 1,5-BTMAPAQ electrolyte. ....	20
Figure S25   Variation of CO <sub>2</sub> and O <sub>2</sub> partial pressure during the electrochemical reduction and oxidation of 1,5-BTMAPAQ in an one bar atmosphere of 87% N <sub>2</sub> , 9.5% CO <sub>2</sub> , and 3.5% O <sub>2</sub> .....	20
Figure S26   Variation of (a) CO <sub>2</sub> and (b) O <sub>2</sub> partial pressure during the electrochemical reduction and oxidation of 1,5-BTMAPAQ in an one bar atmosphere of 77.4% N <sub>2</sub> , 19.5% CO <sub>2</sub> , and 3.1% O <sub>2</sub> .....	21
Figure S27   Variation of CO <sub>2</sub> partial pressure during the electrochemical reduction and oxidation of 1,8-BTMAPAQ in an one bar atmosphere of 87% N <sub>2</sub> , 10% CO <sub>2</sub> , and 3% O <sub>2</sub> . ....	21
<b>References: .....</b>	<b>22</b>

## General experimental procedures

To a 1 L of flame dried Schlenk flask, 40 mmol of dihydroxyanthraquinone, 88 mmol of anhydrous K<sub>2</sub>CO<sub>3</sub>, and 9.5 mmol of KI were suspended in 160 mL of anhydrous DMF. After being stirred under nitrogen for 20 mins, 88 mmol of 3-bromopropyl trimethylammonium bromide was added to the dark suspension. The dark suspension was sealed to prevent ambient moisture, then was vigorously stirred at 100 °C for 16 hours to afford a brownish slurry.

After being cooling down, the slurry was added with 150 mL of ethyl acetate, stirred at room temperature for 30 mins, then filtered to collect the brown cake. The washing procedure was repeated for few times until the filtrate became colorless. The cake was dissolved into methanol, and the solution was filtered to remove insoluble inorganic salts. The filtrate was condensed under vacuo to remove methanol and collect the dark red solid, which was then redissolved in deionized water.

The aqueous quinone solution was then transferred to an anion-exchange resin column prepared in advance to replace bromide with chloride ions. The dark red (bright yellow depending on the concentration) solution was condensed under vacuo to remove water and collect the red solid.

The red solid was re-dissolved in methanol to get the saturated solution, which was then drop-wise added to 200 mL of ethyl acetate and afford precipitates. The precipitates were collected by filtration to get final orange to yellow cakes. The yields range from 85% to 95%.

Among the four BTMAPAQ isomers, the synthesis of 1,8-BTMAPAQ was reported elsewhere.<sup>1</sup>

The syntheses of AQ-1,8-3E-OH and 2,6-D2PEAQ were followed with our previous work without further modification.<sup>2,3</sup>

Structural characterization

<sup>1</sup>H, <sup>13</sup>C NMR spectra were recorded on Varian INOVA 500 spectrometers at 500 MHz. Aliquots were prepared in deuterated water (D<sub>2</sub>O), corresponding NMR spectra were recorded in D<sub>2</sub>O with the residual H<sub>2</sub>O ( $\delta$  4.79 ppm for <sup>1</sup>H NMR).

#### Electrochemical characterizations

Glassy carbon was used as the working electrode for all three-electrode cyclic voltammetry measurements with a 5 mm diameter glassy carbon working electrode, an Ag/AgCl reference electrode (BASi, pre-soaked in 3 M NaCl solution), and a graphite counter electrode. All cyclic voltammetry, linear sweep voltammetry, and chronoamperometry measurements were conducted on Gamry Instruments and CHI Instrument electrochemical analysers.

#### Flow cell assembly

Flow cell experiments were constructed with cell hardware from Fuel Cell Tech (Albuquerque, NM). The flow cell was assembled into a zero-gap flow cell configuration using pyrosealed POCO graphite flow plates with identical interdigitated flow fields. Each electrode was composed of 1 layer of AvCarb HCBA carbon cloth with a 5 cm<sup>2</sup> geometric surface area. Selemion DSV-N was used as the anion exchange membrane. The flow rate was set at 50–70 mL/min. Biologic SP-150e and Gamry Reference 3000 potentiostat was used as our electrochemical workstation. KNF diaphragm pumps were used to circulate electrolytes through the flow fields and electrodes in the cell stack. For some tests, a Cole-Parmer Digital gear pump was used.

Bis((3-trimethylammonio)propyl)ferrocene dichloride (BTMAPFc) and (ferrocenylmethyl)trimethylammonium Chloride (FcNCl) were purchased from TCI-America chemical company. Tetramethyl ammonium chloride, tetrabutylammonium chloride were purchased from Sigma Aldrich. All those chemicals were directly used without further purification.

#### Electrochemical CO<sub>2</sub> capture and release

Flow cells were charged at constant current, followed by voltage holds until current hits the background current values. Then the flow cells were set in rest mode for certain time to complete carbon capture. The cells were discharged at constant current, followed by a voltage hold. After the voltage hold, the battery was set in rest mode to complete CO<sub>2</sub> release. FS4001 MEMS Mass Flow Sensor, LuminOX O<sub>2</sub> sensor (CM-42990), SprintIR CO<sub>2</sub> sensor (GC-0018) were used in our tests.

A stream of feed gas composed of N<sub>2</sub>, CO<sub>2</sub>, and O<sub>2</sub> was introduced to the anthraquinone electrolytes and kept flowing constantly with pre-set partial pressure. The total pressure is 1 bar, and the total flow rate is 11.76 mL/min.

#### The cell testing condition for Fig. 3c is shown below:

During the charge-discharge process, a constant current density of 20 mA/cm<sup>2</sup> was first applied until the voltages approached the pre-set cutoffs. Potential holds were applied at 1.45 V for the charge in pure N<sub>2</sub>, 1.5 V for the charge in 90% N<sub>2</sub> and 10% CO<sub>2</sub>, and 0.05 V for the discharge until the current density decreased to 1 mA/cm<sup>2</sup>.

#### The cell testing conditions for Fig. 4 are shown below:

##### Experiments at different current density:

Flow cells were charged using the constant current specified in each plot (20, 40, 60, 80, 100 mA/cm<sup>2</sup>). This constant current was applied until the charging voltage reached 1.5 V. Afterward, the voltage was held at this value until the current dropped to 5 mA/cm<sup>2</sup>. During discharge, the corresponding constant current (20, 40, 60, 80, 100 mA/cm<sup>2</sup>) was applied until the discharge voltage reached 0.05 V. Afterward, the voltage was held at this value until the current dropped to 1 mA/cm<sup>2</sup>.

##### Experiments at different partial pressures:

For partial pressures of 0.05 bar, 0.1 bar, and 0.2 bar, a constant current of 20 mA/cm<sup>2</sup> was applied until the charging voltage reached 1.3 V. Afterward, the voltage was held at this value until the current dropped to 5 mA/cm<sup>2</sup>. During discharge, a 20 mA/cm<sup>2</sup> constant current was applied until the discharge voltage reached 0.05 V. Afterward, the voltage was held at this value until the current dropped to 1 mA/cm<sup>2</sup>. For the test conducted under a partial pressure of 0.5 bar, the same protocol was used except that the charging voltage was set at 1.1 V instead of 1.3 V. This adjustment was necessary because 1,1'-Bis[3-(trimethylammonio)propyl]ferrocene Dichloride (BTMAPFc) was used instead of ferrocenylmethyltrimethylammonium Chloride (FcNCl) as the posolyte electrolyte (counter reaction), requiring a slightly lower charging voltage.

##### Experiment at 10% – 100% CO<sub>2</sub> purge:

For the tests conducted where the capture occurred in an inlet CO<sub>2</sub> partial pressure of 0.1 bar and release occurred into an inlet CO<sub>2</sub> partial pressure of 1 bar, a constant current of 20 mA/cm<sup>2</sup> was applied until the charging voltage reached 1.4 V. Afterward, the voltage was held at this value until the current dropped to 5 mA/cm<sup>2</sup>. During discharge, the 20 mA/cm<sup>2</sup> constant current was applied until the discharge voltage reached 0.1 V. Afterward, the voltage was held at this value until the current dropped to 1 mA/cm<sup>2</sup>.

Experiment at high concentration:

For the tests conducted at the high concentration of 0.4 M, a constant current of 20 mA/cm<sup>2</sup> was applied until the charging voltage reached 1.4 V. Afterward, the voltage was held at this value until the current dropped to 5 mA/cm<sup>2</sup>. During discharge, the 20 mA/cm<sup>2</sup> constant current was applied until the discharge voltage reached 0.1 V. Afterward, the voltage was held at this value until the current dropped to 1 mA/cm<sup>2</sup>.

## Solubility of anthraquinones in different stages in different supporting salts

**Table S1 | Solubility behavior of anthraquinones in different supporting salts.**

Compound	Q solubility @ pH 7	0.1 M Q(CO <sub>2</sub> ) <sub>2</sub> <sup>2-</sup>		
		+ 1 M K <sup>+</sup> /Na <sup>+</sup>	+ 1 M TBA <sup>+</sup>	+ 1 M TMA <sup>+</sup>
AQDS	0.3	insoluble	insoluble	soluble
AQ-1,8-3E-OH	2.2	insoluble	soluble	insoluble
2,6-D2PEAQ	2.0	insoluble	soluble	insoluble
1,4-BTMAPAQ	1.0	soluble		
1,5-BTMAPAQ	1.3	soluble		
1,8-BTMAPAQ	1.0	insoluble	soluble	
2,6-BTMAPAQ	< 0.1	N/A		

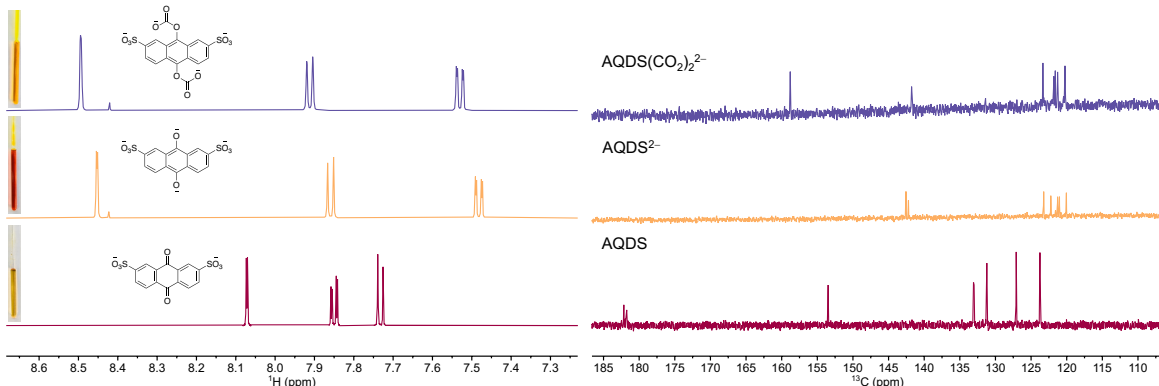


**Figure S1 | <sup>1</sup>H and <sup>13</sup>C NMR spectra of 0.1 M AQDS, AQDS<sup>2-</sup>, AQDS(CO<sub>2</sub>)<sub>2</sub><sup>2-</sup> 1 M TMACl D<sub>2</sub>O solutions.** The corresponding color is yellow, red, and bright yellow.

## Compatibility issue between bulky alkylammonium cation ( $\text{TBA}^+$ ) and cation-exchange membrane

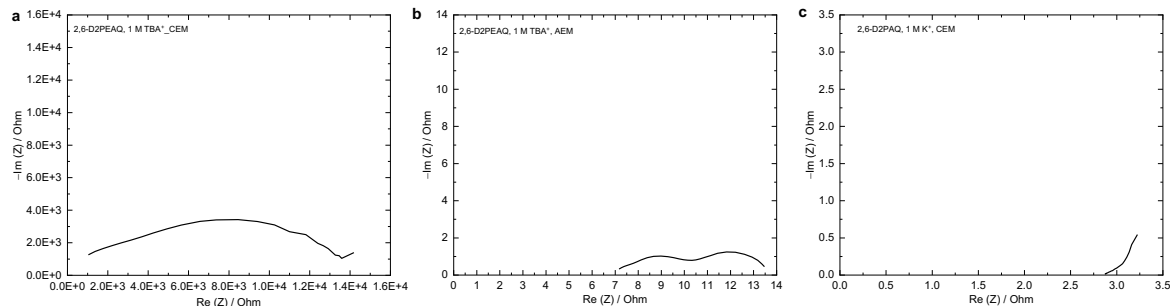


**Figure S2 | Electrochemical impedance spectroscopy (EIS) measurement of 2,6-D2PEAQ flow cells.** Alternating current area-specific resistance of the cells were determined via high-frequency EIS. (a) 0.1 M 2,6-D2PEAQ, 1 M  $\text{TBA}^+$  | 0.1 M  $\text{Fe}(\text{CN})_6^{3/4-}$ , 1 M  $\text{TBA}^+$ , where a cation-exchange membrane, Nafion 212, was used to separate the electrolytes. (b) 0.1 M 2,6-D2PEAQ, 1 M  $\text{TBA}^+$  | 0.1 M  $\text{Fe}(\text{CN})_6^{3/4-}$ , 1 M  $\text{TBA}^+$ , where an anion-exchange membrane, DSV-N, was used to separate the electrolytes. (c) 0.1 M 2,6-D2PEAQ, 1 M  $\text{K}^+$  | 0.1 M  $\text{Fe}(\text{CN})_6^{3/4-}$ , 1 M  $\text{K}^+$ , where a cation-exchange membrane, Nafion 212 was used to separate the electrolytes. The impedance measurements were conducted at 0% of state of charge. The geographic area of electrode is  $5 \text{ cm}^2$ .

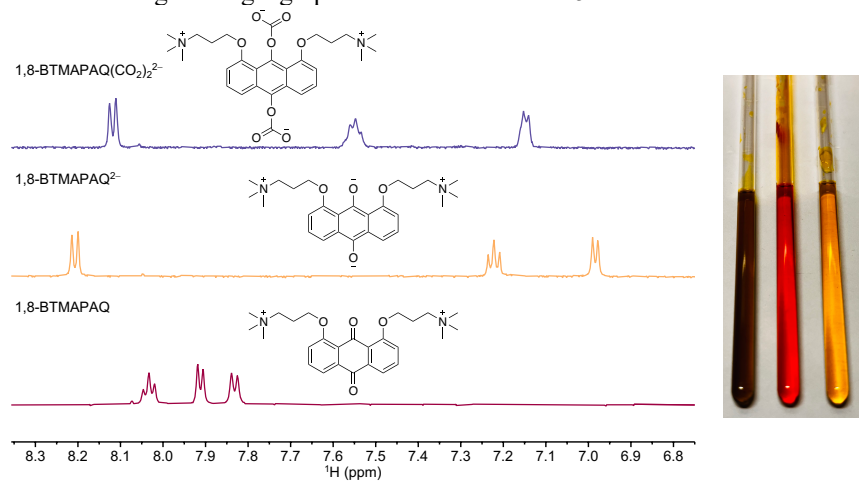


**Figure S3 | Stacked  $^1\text{H}$  NMR spectra of 1,8-BTMAPAQ in three states.** Bottom to top: (1): 0.1 M 1,8-BTMAPAQ in 1 M  $\text{TBA}^+$ ; (2) 0.1 M reduced 1,8-BTMAPAQ in 1 M  $\text{TBA}^+$ ; (3) 0.1 M reduced 1,8-BTMAPAQ with saturated  $\text{CO}_2$  in 1 M  $\text{TBA}^+$ . The corresponding color is brown, red, and bright yellow. We selected 6.7 ppm–8.4 ppm to highlight the chemical shifts in the aromatic region.

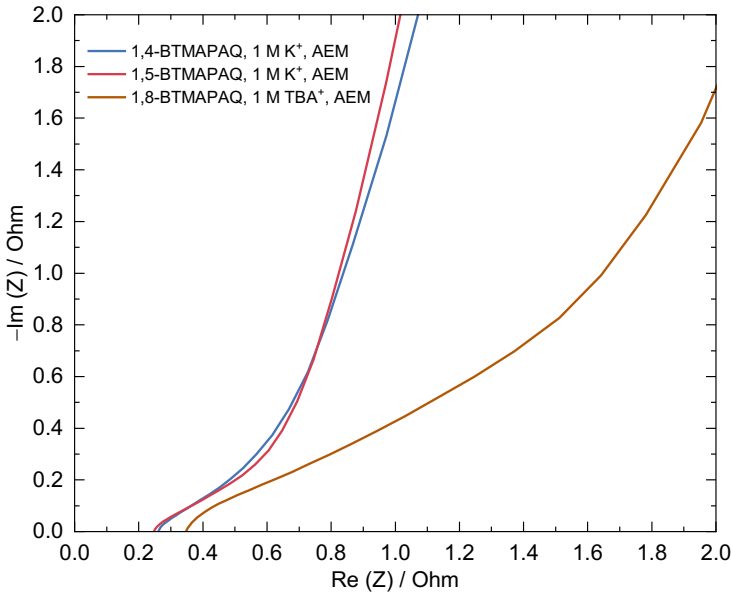


**Figure S4 | Electrochemical impedance spectroscopy (EIS) measurement of 0.1 M BTMAPAQ | 0.1 M FeNCl flow cells**, where an anion-exchange membrane, DSV-N, was used to separate the electrolytes. The supporting salt of 1,4-, 1,5-BTMAPAQ electrolytes is 1 M KCl, whereas the supporting salt of 0.1 M 1,8-BTMAPAQ electrolyte is 1 M TBACl. The impedance measurements were conducted at 0% of state of charge. The geographic area of electrode is 5 cm<sup>2</sup>.

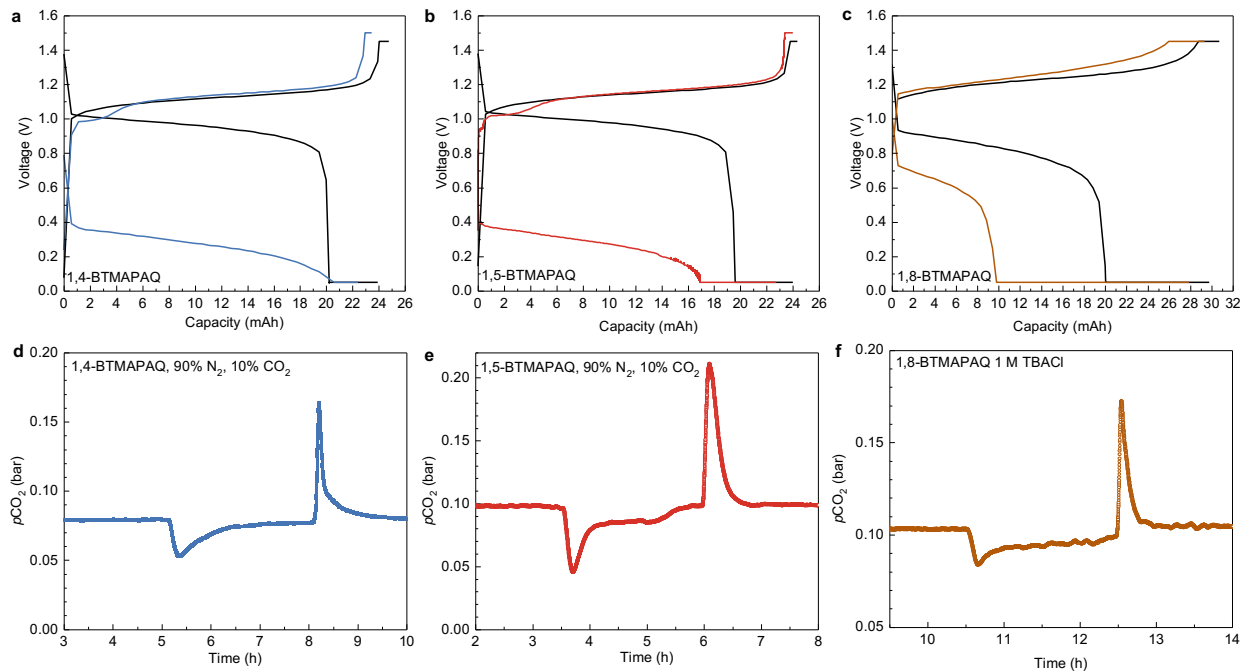


**Figure S5 | Voltage profiles and CO<sub>2</sub> partial pressure during the electrochemical reduction and oxidation of BTMAPAQs.** Electrolyte composition: 5 mL 0.1 M 1,4-, 1,5-BTMAPAQs, 1 M KCl vs. 40 mL 0.1 M FeNCl, 1 M KCl. 5 mL 0.1 M 1,8-BTMAPAQ, 1 M TBACl vs. 40 mL 0.1 M FeNCl, 1 M TBACl. Constant current (40 mA/cm<sup>2</sup>) was followed with potential holds.

## Chemical CO<sub>2</sub> capture, release, and sequestration procedure in the absence of O<sub>2</sub>

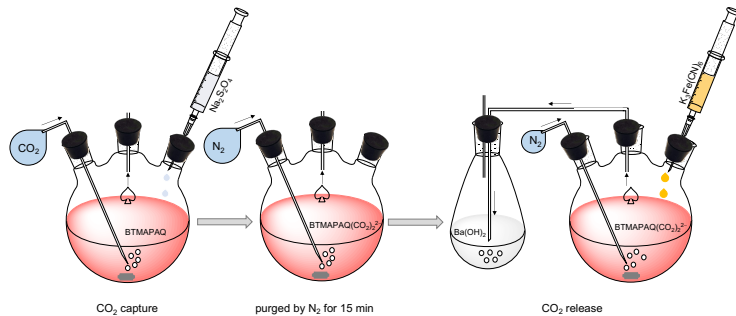


**Figure S6 | Chemically induced CO<sub>2</sub> capture, release, and sequestration.** Capture: AQ + S<sub>2</sub>O<sub>4</sub><sup>2-</sup> + 2CO<sub>2</sub> + 2OH<sup>-</sup> → AQ(CO<sub>2</sub>)<sub>2</sub><sup>2-</sup> + 2HSO<sub>3</sub><sup>-</sup> (step 1). Release: AQ(CO<sub>2</sub>)<sub>2</sub><sup>2-</sup> + 2Fe(CN)<sub>6</sub><sup>3-</sup> → AQ + 2Fe(CN)<sub>6</sub><sup>4-</sup> + 2CO<sub>2</sub>↑ (step 2).

Sequestration: CO<sub>2</sub> + Ba(OH)<sub>2</sub> → BaCO<sub>3</sub>↓ + H<sub>2</sub>O (step 3).

Step 1: with continuous CO<sub>2</sub> purging, the flask containing 0.1 M 1,8-BTMAPAQ, 1 M TBACl solution was added with a saturated aqueous solution containing two equivalents of NaOH and one equivalent of Na<sub>2</sub>S<sub>2</sub>O<sub>4</sub>, forming the hemi carbonate [AQ(CO<sub>2</sub>)<sub>2</sub><sup>2-</sup>].

Step 2: the solution was vigorously stirred in N<sub>2</sub> for 15 mins followed with 15-min N<sub>2</sub> purging.

Step 3: with continuous N<sub>2</sub> purging, the flask containing quinone solution was connected with another flask containing saturated Ba(OH)<sub>2</sub> solution prepared in advance under N<sub>2</sub>. With N<sub>2</sub> purging, a saturated aqueous solution containing two equivalents of K<sub>4</sub>Fe(CN)<sub>6</sub> was dropwise added to the quinone solution, generating CO<sub>2</sub> bubbles. The generated CO<sub>2</sub> was carried by N<sub>2</sub> to the Ba(OH)<sub>2</sub> flask, immediately forming cloudy BaCO<sub>3</sub>.

The resulting suspension was centrifuged to collect the precipitates which were then dried in an oven completely until the dry mass becomes constant. The CO<sub>2</sub> capture capacity was calculated from the dry mass of BaCO<sub>3</sub>. The power was cooled down in a desiccant then quickly weighed in a precision balance to obtain the dry mass.

BTMAPAQ chemical reduction/oxidation induced CO<sub>2</sub> capture/release followed with sequestration were designed to determine the carbon capture capacity. We found that one 1,8-BTMAPAQ molecule can capture and release two CO<sub>2</sub> molecules in the absence of oxygen.

## Electrochemical CO<sub>2</sub> capture in O<sub>2</sub>-free environment

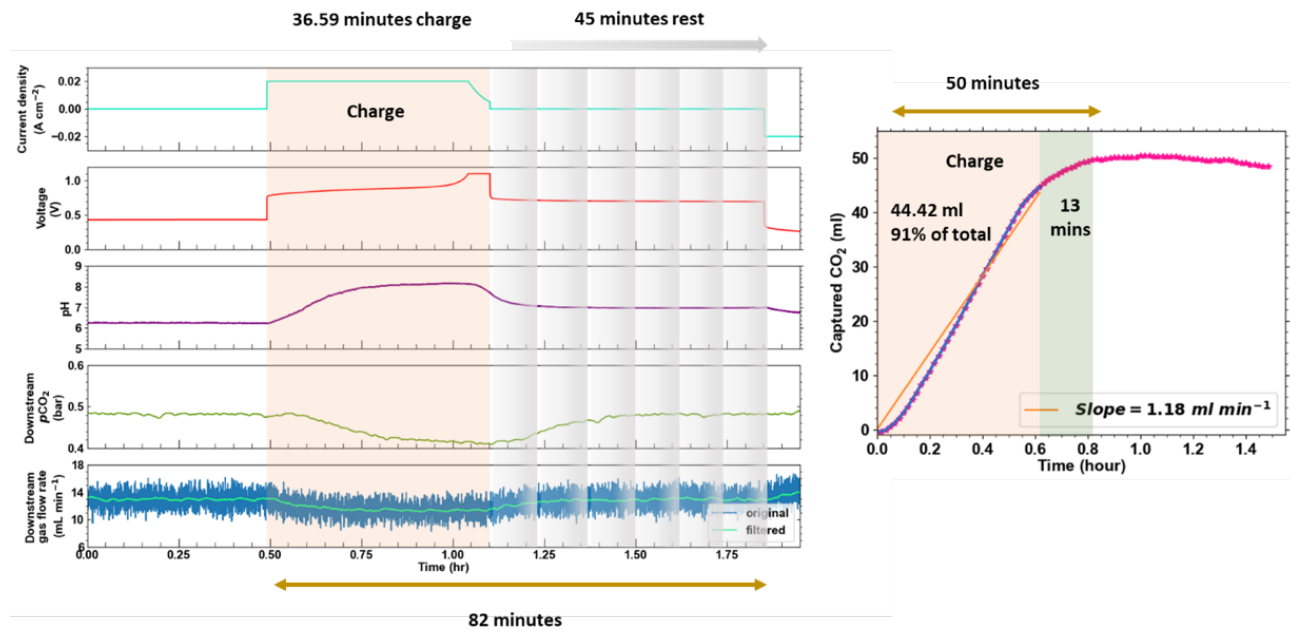


**Figure S7 | Cumulative CO<sub>2</sub> captured during the charge and rest time for the fourth cycle of Figure 4a 0.5 bar CO<sub>2</sub> experiment.** The figure demonstrates the total time needed for the complete capture of CO<sub>2</sub> for the conditions described in Figure 4a for the 0.5 bar CO<sub>2</sub> experiment.

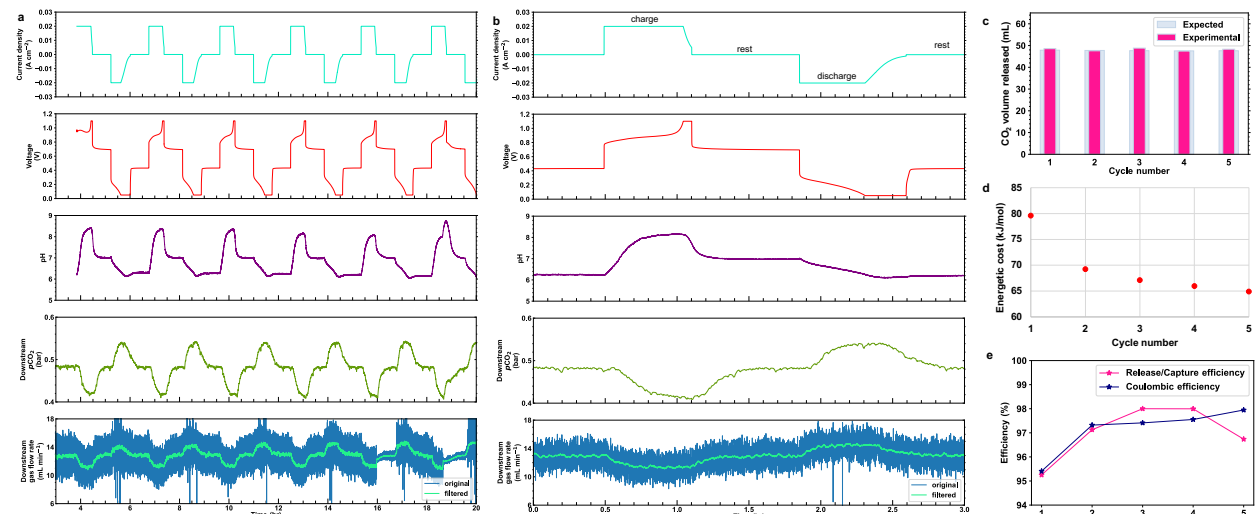


**Figure S8 | CO<sub>2</sub> capture and release cycling in a flow cell** comprising 10 mL of 0.115 M 1,5-BTMAPAQ in 1 M KCl (negolyte) and 40 mL of 0.1 M BTMAPFc in 1 M KCl (posolyte) at 20 mA/cm<sup>2</sup>. The partial pressure of CO<sub>2</sub> is set to  $\approx$ 0.5 bar throughout the experiment. Plot on the left (a) presents (from top to bottom): current density, voltage, pH of the negolyte, the percentage of N<sub>2</sub> and CO<sub>2</sub> in the upstream source gas, downstream CO<sub>2</sub> partial pressure and the downstream total gas flow rate. The initial gas flow rate is set to 11.76 mL/min. Plot on the right top (b) shows zoomed-in data of the fourth cycle. Plots on the bottom right (c) presents the volume of the CO<sub>2</sub> gas (in mL) calculated from the deviation from the baseline flow rate during the battery discharge and rest period. The second plot on the bottom right demonstrates the energy (d) required for each cycle of capture and release (kJ/mol) and the coulombic efficiencies (e) and release/capture efficiencies per cycle. Bis((3-trimethylammonio)propyl)ferrocene dichloride (BTMAPFc) was purchased from TCI-America chemical company.

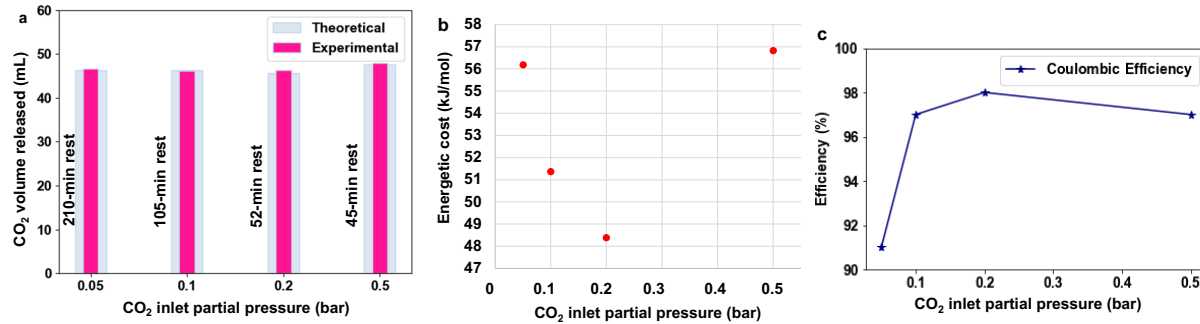


**Figure S9 | CO<sub>2</sub> capture and release using different CO<sub>2</sub> partial pressure values in a flow cell comprising 12 mL of 0.115 M 1,5-BTMAPAQ in 1 M KCl (negolyte) and 40 mL of 0.2 M FcNCl in 1 M KCl (posolyte) at 20 mA/cm<sup>2</sup>. The partial pressure of CO<sub>2</sub> is changing from 0.05 bar to 0.5 bar throughout the experiment. Plot on the top (a) shows the volume of the CO<sub>2</sub> gas (in mL) calculated from the deviation from the baseline flow rate during the battery discharge and rest period. The plot on the bottom demonstrates the average energy (b for 2 cycles) required for the capture and release of CO<sub>2</sub> and the coulombic efficiencies (c) using different CO<sub>2</sub> partial pressure values. Two CO<sub>2</sub> molecules were captured by one 1,5-BTMAPAQ with energetic cost of 48–57 kJ/molCO<sub>2</sub> at 20 mA/cm<sup>2</sup>. (Ferrocenylmethyl)trimethylammonium Chloride (FcNCl) was purchased from TCI-America chemical company.**

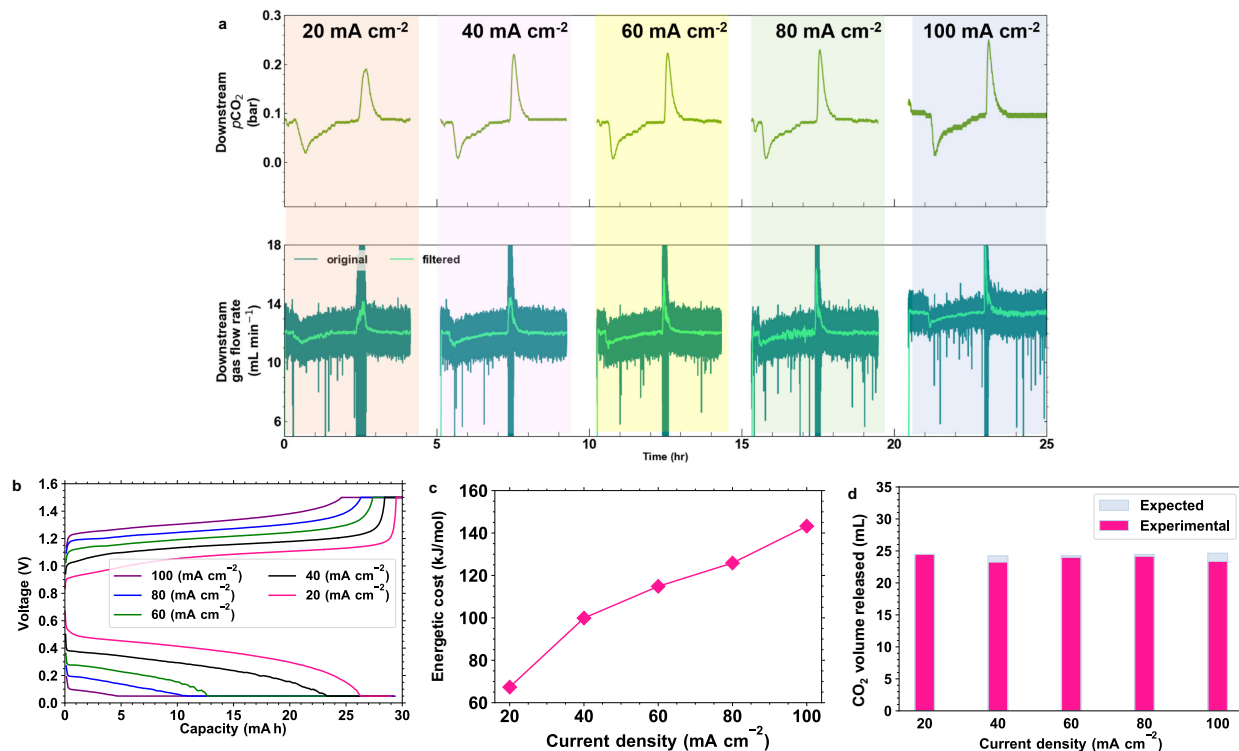


**Figure S10 | CO<sub>2</sub> capture and release cycling at different current densities (20, 40, 60, 80, 100 mA/cm<sup>2</sup>) in inlet CO<sub>2</sub> partial pressure of 0.1 and 0.5 bar in a flow cell comprising 10 mL of 0.057 M 1,5-BTMAPAQ in 1 M KCl (negolyte) and 40 mL of 0.2 M FcNCl in 1 M KCl (posolyte). Plot on the top left (a) presents the downstream CO<sub>2</sub> partial pressure and the downstream total gas flow rate. The initial gas flow rate is set to 11.76 mL/min. The plot on the top right (b) demonstrates the voltage versus capacity for each current density. (c) Plot shows the volume of the CO<sub>2</sub> gas (in mL) calculated from the deviation from the baseline flow rate during the battery discharge and rest period. (d) Plot shows the energetic cost of one charge and discharge per moles of released CO<sub>2</sub> for each current density tested.**

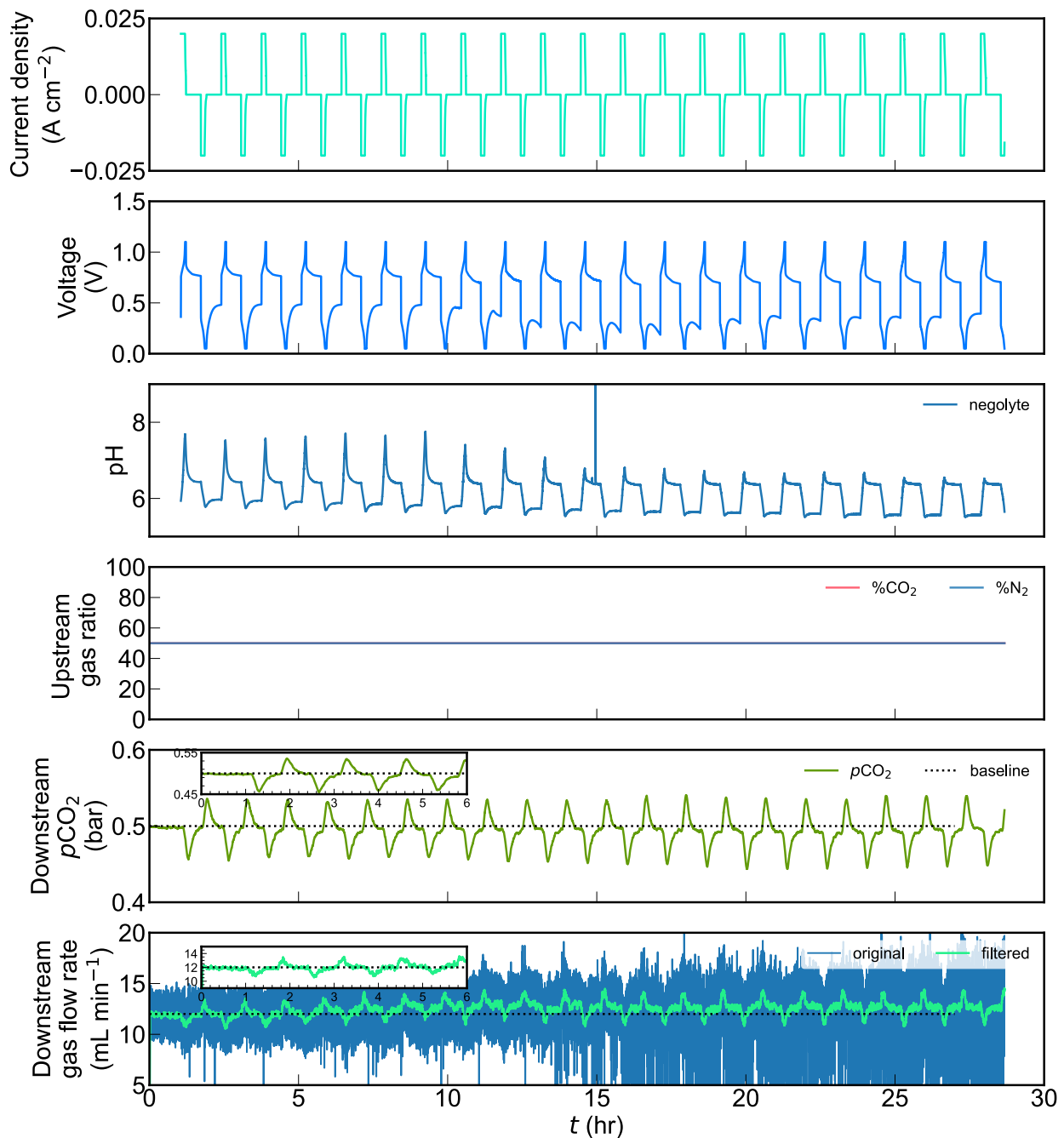


**Figure S11 |  $\text{CO}_2$  capture and release cycling at a current density of  $20 \text{ mA/cm}^2$  in inlet  $\text{CO}_2$  partial pressure of  $0.5 \text{ bar}$  in a flow cell comprising  $10 \text{ mL}$  of  $0.057 \text{ M}$  1,5-BTMAPAQ in  $1 \text{ M KCl}$  (negolyte) and  $40 \text{ mL}$  of  $0.2 \text{ M}$  FcNCl in  $1 \text{ M KCl}$  (posolyte). Plots show the extended 21-cycle performance.**

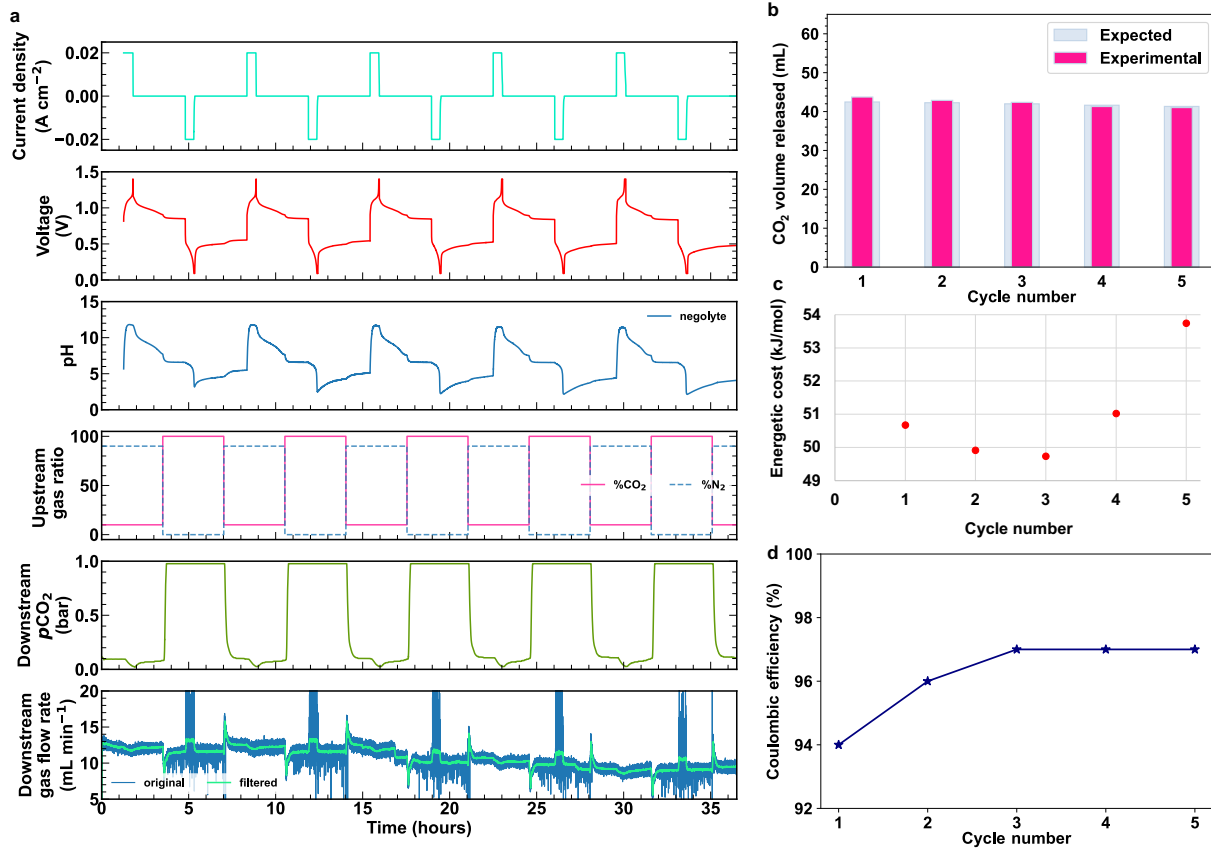


**Figure S12 |** **CO<sub>2</sub> capture and release cycling where the capture occurs in an inlet CO<sub>2</sub> partial pressure of 0.1 bar and the release occur in an inlet CO<sub>2</sub> partial pressure of 1 bar in a flow cell comprising 12 mL of 0.115 M 1,5-BTMAPAQ in 1 M KCl (negolyte) and 40 mL of 0.2 M FeNCl in 1 M KCl (posolyte) at 20 mA/cm<sup>2</sup>.** Plot on the left (a) presents (from top to bottom): current density, voltage, pH of the negolyte, the percentage of N<sub>2</sub> and CO<sub>2</sub> in the upstream source gas, downstream CO<sub>2</sub> partial pressure and the downstream total gas flow rate. The initial gas flow rate is set to 11.76 mL/min. Plot on the right top (b) shows the volume of the CO<sub>2</sub> gas (in mL) calculated from the deviation from the baseline flow rate during the battery discharge and rest period. The plot on the bottom right demonstrates the energy (c) required for the capture and release of CO<sub>2</sub> in each cycler and the coulombic efficiency (d) for several cycles.

### Concentrated cell test

A concentrated flow cell comprising 10 mL 0.4 M 1,5-BTMAPAQ and 40 mL 0.9 M FeNCl was assembled and tested. The cell was charged and discharged at 20 mA/cm<sup>2</sup> with no potential holds. The coulombic efficiency is 77% and the discharge capacity is 632.42 C. The experimental volume of released CO<sub>2</sub> is 148 mL which is close to the theoretical volume of released CO<sub>2</sub> (147 mL). The corresponding energetic cost is 90 kJ/molCO<sub>2</sub>.

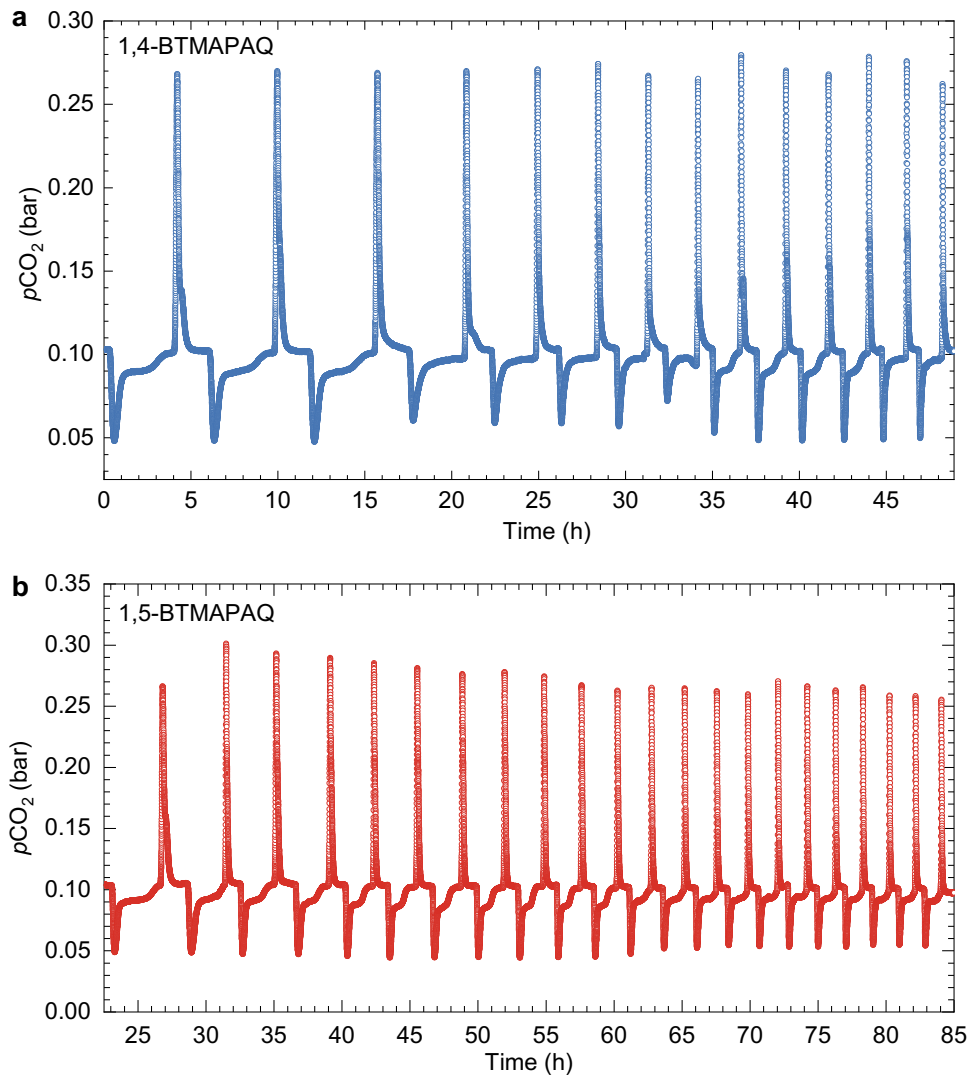


**Figure S13 | CO<sub>2</sub> partial pressure changes over the electrochemical reduction and oxidation cycling of 1,4- and 1,5-BTMAPAQs.** Electrolyte composition: 5 mL 0.1 M 1,4-, 1,5-BTMAPAQs, 1 M KCl vs. 40 mL 0.1 M FeNCl, 1 M KCl. Constant current (40 mA/cm<sup>2</sup>) was followed with potential holds.

## Oxygen sensitivity of reduced anthraquinones [H<sub>2</sub>Q, HQ<sup>-</sup>, Q<sup>2-</sup>, HQ(CO<sub>2</sub>)<sup>-</sup>, and Q(CO<sub>2</sub>)<sub>2</sub><sup>2-</sup>]

CO<sub>2</sub> and O<sub>2</sub> account for ~10% and <5% in coal fired flue gas; ~0.04% (400 ppm) and 21% in air. Therefore, it is important to evaluate the oxygen effect of active species if were used for CO<sub>2</sub> capture.

Instead of exhaustively evaluating the oxygen sensitivity of each species, we mainly investigated two states, *i.e.*, fully reduced state with no chemisorbed CO<sub>2</sub> in which the most dominant and O<sub>2</sub>-sensitive species is Q<sup>2-</sup>; fully reduced state with chemisorbed CO<sub>2</sub> in which the most dominant species is Q(CO<sub>2</sub>)<sub>2</sub><sup>2-</sup>. The quinones in dissolved D<sub>2</sub>O were chemically reduced and stored in air-tight J-Young NMR tubes, named as Q<sup>2-</sup>; the quinones dissolved in D<sub>2</sub>O were chemically reduced, introduced with CO<sub>2</sub>, and stored in air-tight J-Young NMR tubes, named as Q(CO<sub>2</sub>)<sub>2</sub><sup>2-</sup>. The <sup>1</sup>H NMR spectra of two group samples were first collected in air-free environment. Subsequently, the samples were intentionally subject to air exposure, then tracked by <sup>1</sup>H NMR over the course of several days.

The oxygen sensitivity of 1,4-, 1,5-, 1,8-BTMAPAQ at states of Q<sup>2-</sup> and Q(CO<sub>2</sub>)<sub>2</sub><sup>2-</sup> was first evaluated by tracking their <sup>1</sup>H NMR followed with quantitative analyses of the aromatic peak areas in spectra. The <sup>1</sup>H NMRs of Q(CO<sub>2</sub>)<sub>2</sub><sup>2-</sup> for AQDS, 2,6-D2PEAQ, and AQ-1,8-3E-OH were also tracked even though the use of tetra-alkyl ammonium salts to dissolve Q(CO<sub>2</sub>)<sub>2</sub><sup>2-</sup> makes them unlikely to be used for electrochemical CO<sub>2</sub> capture. It is worth noting that exposing the reduced species in J-Young tubes to air is significantly different from practical application scenarios where huge amount of air would be vigorously pulled into electrolytes, we expect to extract the relative oxygen sensitivity trend from the comparison of those <sup>1</sup>H NMR spectra. The detailed analyses and comparison can be found below. Q<sup>2-</sup> is generally more oxygen-sensitive than Q(CO<sub>2</sub>)<sub>2</sub><sup>2-</sup>, which is consistent with the right shifted anodic peaks observed in the CV results. Among the measured anthraquinones, 1,8-BTMAPAQ appears to be the least oxygen-sensitive, followed by 1,5- and 1,4-BTMAPAQ. Note that, 1 M TBACl was used for 1,8-BTMAPAQ electrolyte preparation, the resulting electrolyte become viscous, which might be the main reason being the least oxygen-sensitive. Molecular decomposition occurred in 1,8-BTMAPAQ<sup>2-</sup>, indicated by the appearance of side peaks over the course of air exposure.

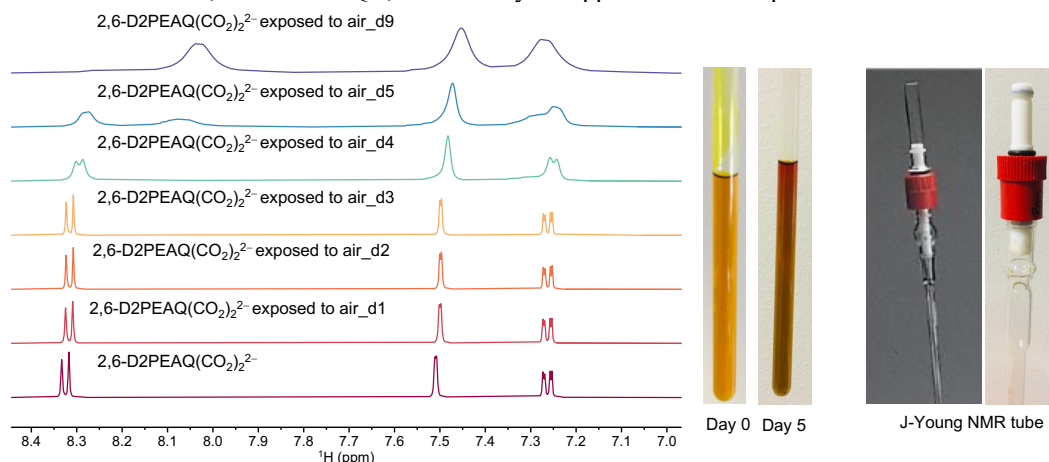


**Figure S14 | <sup>1</sup>H NMR tracking of chemically synthesized 0.1 M 2,6-D2PEAQ(CO<sub>2</sub>)<sub>2</sub><sup>2-</sup> in 1 M TBABr D<sub>2</sub>O over days while air was gradually introduced.**

0.1 M 2,6-D2PEAQ<sup>2-</sup> in 1 M tetra-n-butylammonium bromide (TBABr) D<sub>2</sub>O solution was added to excess dry ice to form 2,6-D2PEAQ(CO<sub>2</sub>)<sub>2</sub><sup>2-</sup> and stored in a J-Young NMR tube. The <sup>1</sup>H NMR of 2,6-D2PEAQ(CO<sub>2</sub>)<sub>2</sub><sup>2-</sup> solution was periodically tracked over days. A tightly sealed J-Young NMR tube can well isolate the stored solution from air. One day-0, the <sup>1</sup>H NMR spectrum was taken in the air-tight J-Young NMR tube. From day-1, the red cap (shown in the pictures) was loosened and the white PTFE tip detached from the inner wall of the J-Young tube, allowing air to gradually diffuse into the solution and oxidize 2,6-D2PEAQ(CO<sub>2</sub>)<sub>2</sub><sup>2-</sup>. As can be seen from the stacked <sup>1</sup>H NMR spectra, in the first three days, the aromatic peaks of 2,6-D2PEAQ(CO<sub>2</sub>)<sub>2</sub><sup>2-</sup> show clear splitting, indicating most of 2,6-D2PEAQ(CO<sub>2</sub>)<sub>2</sub><sup>2-</sup> remained intact; from day-4, the aromatic peaks became broader and shifted, which is due to the occurrence of semi-radical anions, the partially oxidized species. 2,6-D2PEAQ(CO<sub>2</sub>)<sub>2</sub><sup>2-</sup> was gradually oxidized by molecular oxygen, forming oxidized species and hydroxide ions, which altered the pH of the solution. The color of the solution turned from bright yellow on day-0 to brown reddish on day-5 which is close to the color of the pristine 2,6-D2PEAQ solution (Figure 2a), implying that oxidation happened over the course of air exposure.

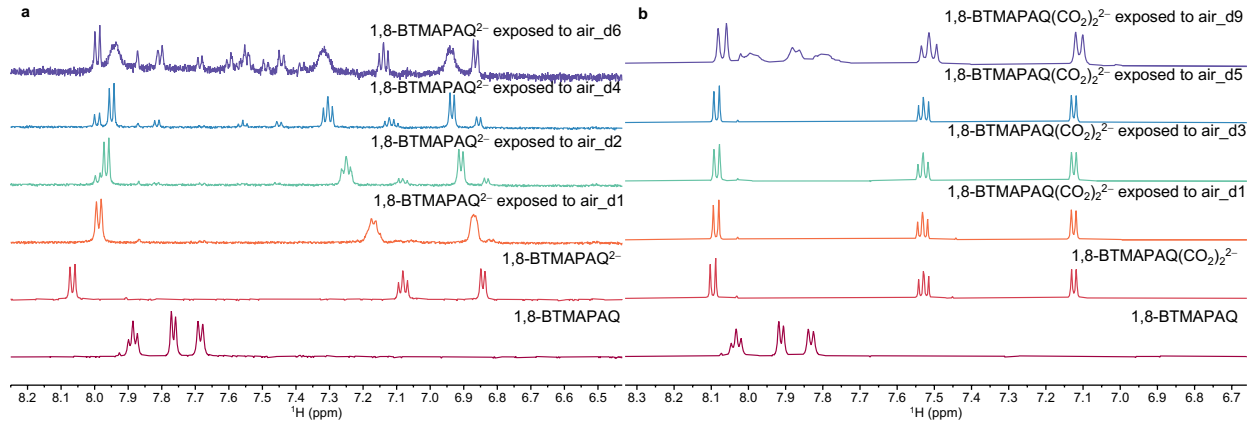


**Figure S15 | <sup>1</sup>H NMR tracking of chemically synthesized 0.1 M 1,8-BTMAPAQ<sup>2-</sup> (a) and 0.1 M 1,8-BTMAPAQ(CO<sub>2</sub>)<sup>2-</sup> (b) in 1 M TBABr D<sub>2</sub>O over days while air was gradually introduced.**

0.1 M 1,8-BTMAPAQ, 1 M TBABr in D<sub>2</sub>O was first chemically reduced by a stoichiometric amount of Na<sub>2</sub>S<sub>2</sub>O<sub>4</sub> with and without excess dry ice. The two samples were stored in two separate J-Young NMR tubes for day-0 tests. After that, the caps of J-Young NMR tubes were loosened up so that air can slowly diffuse into the solutions. The <sup>1</sup>H NMR spectrum of 0.1 M 1,8-BTMAPAQ was taken to serve as a control sample. On day-4 and day-6, some new peaks other than the peaks from 1,8-BTMAPAQ appear in the sample of 1,8-BTMAPAQ<sup>2-</sup>, suggesting that 1,8-BTMAPAQ<sup>2-</sup> is not structurally stable and molecular decomposition happened. On day-9, the sample of 1,8-BTMAPAQ(CO<sub>2</sub>)<sup>2-</sup> showed the three sets of broad peaks between 7.7 ppm and 8.05 ppm which are similar to those in 1,8-BTMAPAQ, suggesting the hemi carbonate (quinone-CO<sub>2</sub> adduct) was slowly oxidized back to 1,8-BTMAPAQ.

As indicated in Figure 3a, the oxidation potentials of 1,8-BTMAPAQ<sup>2-</sup> and 1,8-BTMAPAQ(CO<sub>2</sub>)<sup>2-</sup> are -0.38 V and 0.12 V vs. SHE, which are lower than the reduction potential of O<sub>2</sub> (0.28 V vs. SHE) at pH 7. The relatively good oxygen resistance over days might be attributed to the addition of 1 M TBABr salt, which made the electrolyte more viscous, slowing down the dissolution of oxygen in the solution.

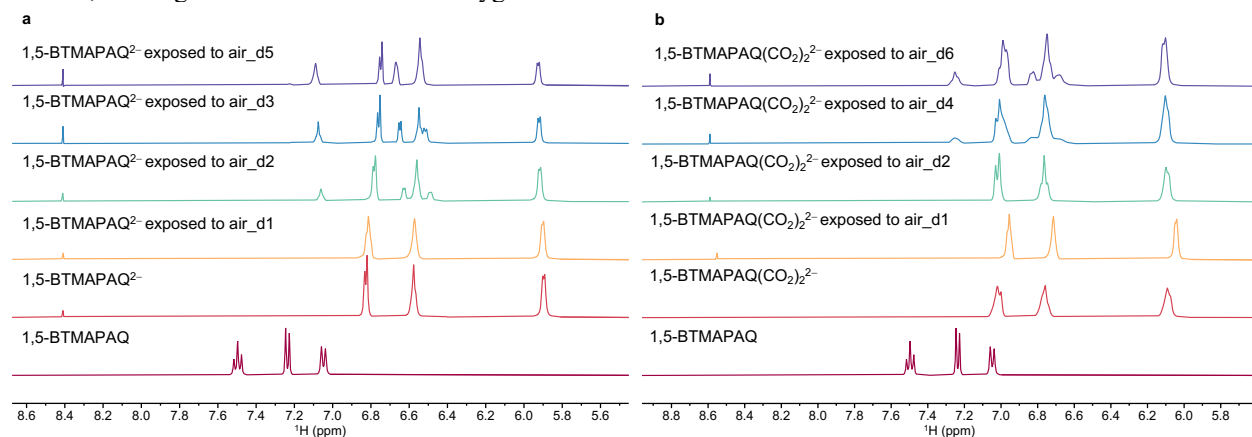


**Figure S16 | <sup>1</sup>H NMR tracking of chemically synthesized 0.1 M 1,5-BTMAPAQ<sup>2-</sup> (a) and 0.1 M 1,5-BTMAPAQ(CO<sub>2</sub>)<sup>2-</sup> (b) in 1 M KCl D<sub>2</sub>O over days while air was gradually introduced.**

The 1,5-BTMAPAQ<sup>2-</sup> and 1,5-BTMAPAQ(CO<sub>2</sub>)<sup>2-</sup> were chemically synthesized and stored in J-Young NMR tubes by following the same methods described for the preparation of 1,8-BTMAPAQ<sup>2-</sup> and 1,8-BTMAPAQ(CO<sub>2</sub>)<sup>2-</sup>. The only difference is using 1 M KCl as the supporting salt instead of 1 M TBABr. The former one is more preferred, as KCl is much smaller in size and much cheaper than tetra-alkyl ammonium salts.

After integrating the characteristic peak area from 1,5-BTMAPAQ, we found 23.6%, 37.0%, and 47.4% of 1,5-BTMAPAQ<sup>2-</sup> were converted to the oxidized form on day-2, day-3, and day-5; whereas 15.0% and 22.3% of 1,5-BTMAPAQ(CO<sub>2</sub>)<sup>2-</sup> were converted to the oxidized form on day-4 and day-6, suggesting 1,5-BTMAPAQ<sup>2-</sup> is more oxygen-sensitive than 1,5-BTMAPAQ(CO<sub>2</sub>)<sup>2-</sup>.

In Figure 3a, the oxidation potentials of 1,5-BTMAPAQ<sup>2-</sup> and 1,5-BTMAPAQ(CO<sub>2</sub>)<sub>2</sub><sup>2-</sup> are -0.38 V and 0.27 V vs. SHE, respectively. The latter one is quite close to the reduction potential (0.28 V vs. SHE) of O<sub>2</sub> at pH 7. It is thus reasonable to see good oxygen resistance from 1,5-BTMAPAQ(CO<sub>2</sub>)<sub>2</sub><sup>2-</sup>.

Unlike 1 M TBABr was used for 1,8-BTMAPAQ electrolytes, 1 M KCl was used for 1,5-BTMAPAQ electrolytes, the electrolytes have low viscosity and high oxygen solubility, that may explain why 1,5-BTMAPAQ<sup>2-</sup> and 1,5-BTMAPAQ(CO<sub>2</sub>)<sub>2</sub><sup>2-</sup> appear to be more oxygen sensitive than their 1,8-isomers (Figure S5).

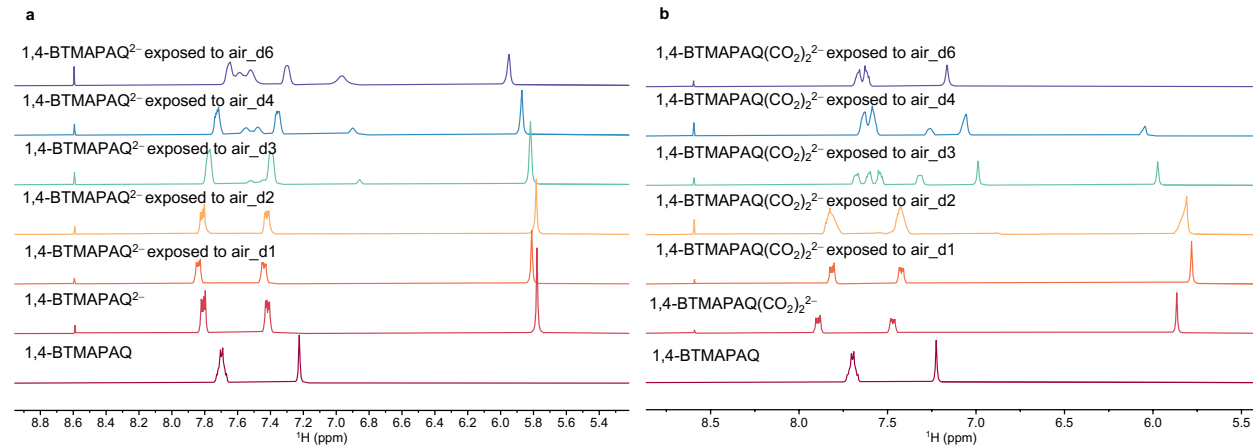


**Figure S17 | <sup>1</sup>H NMR tracking of chemically synthesized 0.1 M 1,4-BTMAPAQ<sup>2-</sup> (a) and 0.1 M 1,4-BTMAPAQ(CO<sub>2</sub>)<sub>2</sub><sup>2-</sup> (b) in 1 M KCl D<sub>2</sub>O over days while air was gradually introduced.**

1,4-BTMAPAQ<sup>2-</sup> and 1,4-BTMAPAQ(CO<sub>2</sub>)<sub>2</sub><sup>2-</sup> were chemically synthesized and stored in J-Young NMR tubes by following the same methods described for the preparation of 1,5-BTMAPAQ<sup>2-</sup> and 1,5-BTMAPAQ(CO<sub>2</sub>)<sub>2</sub><sup>2-</sup>.

After integrating the characteristic aromatic peak area from 1,4-BTMAPAQ, we found 11.3%, 27.6%, and 50% of 1,4-BTMAPAQ<sup>2-</sup> was converted to the oxidized form on day-3, day-4, and day-6; whereas, 51.5%, 73.0%, and 98.0% of 1,4-BTMAPAQ(CO<sub>2</sub>)<sub>2</sub><sup>2-</sup> was converted to the oxidized form on day-3, day-4, and day-6.

The oxidation potentials of 1,4-BTMAPAQ<sup>2-</sup> and 1,4-BTMAPAQ(CO<sub>2</sub>)<sub>2</sub><sup>2-</sup> are -0.36V and 0.23 V vs. SHE respectively; both are lower than the reduction potential of O<sub>2</sub> at pH 7. From the tracked <sup>1</sup>H NMR peak integral comparison, 1,4-BTMAPAQ(CO<sub>2</sub>)<sub>2</sub><sup>2-</sup> seems to be more oxygen sensitive than 1,4-BTMAPAQ<sup>2-</sup>, although the former one has a higher oxidation potential (Figure 3a). A plausible explanation is that reaction kinetics between 1,4-BTMAPAQ(CO<sub>2</sub>)<sub>2</sub><sup>2-</sup> and O<sub>2</sub> is faster than the kinetics between 1,4-BTMAPAQ<sup>2-</sup> and O<sub>2</sub>.

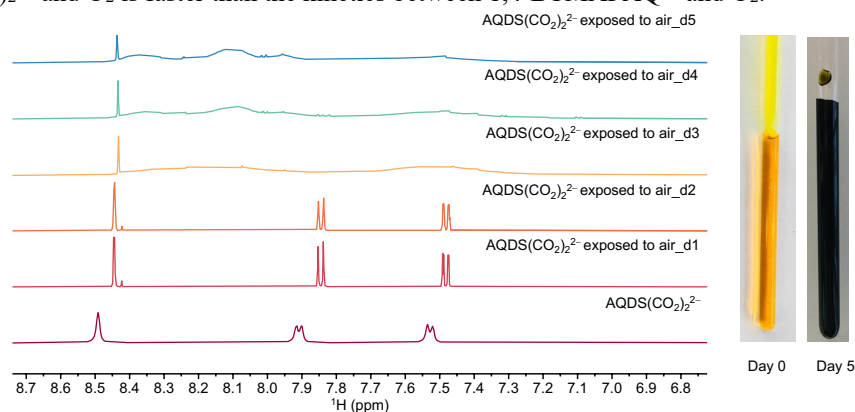


**Figure S18 | <sup>1</sup>H NMR tracking of chemically synthesized 0.1 M AQDS(CO<sub>2</sub>)<sub>2</sub><sup>2-</sup> in 1 M TMACl D<sub>2</sub>O over days while air was gradually introduced.**

The oxygen-sensitivity of 0.1 M AQDS(CO<sub>2</sub>)<sub>2</sub><sup>2-</sup> in 1 M tetramethylammonium chloride (TMACl) D<sub>2</sub>O solution was tracked by <sup>1</sup>H NMR periodically. The solution was prepared by mixing chemically prepared AQDS<sup>2-</sup> with dry ice and stored in a J-Young NMR tube. The day-0 spectrum was taken in an air-tight J-Young NMR tube. From day-1, the cap was loosened, and air was gradually introduced to the solution. As shown in the stacked <sup>1</sup>H NMR spectra, the spectra maintained the same for the first two days, then the peaks become broader from day-3, indicating the coexistence of the oxidized, reduced, and intermediate states of AQDS. The color of the sample on day-5 became dark

green, as opposite to the bright yellow on day-0, suggesting that oxidation happened when the solution was exposed to air over days.

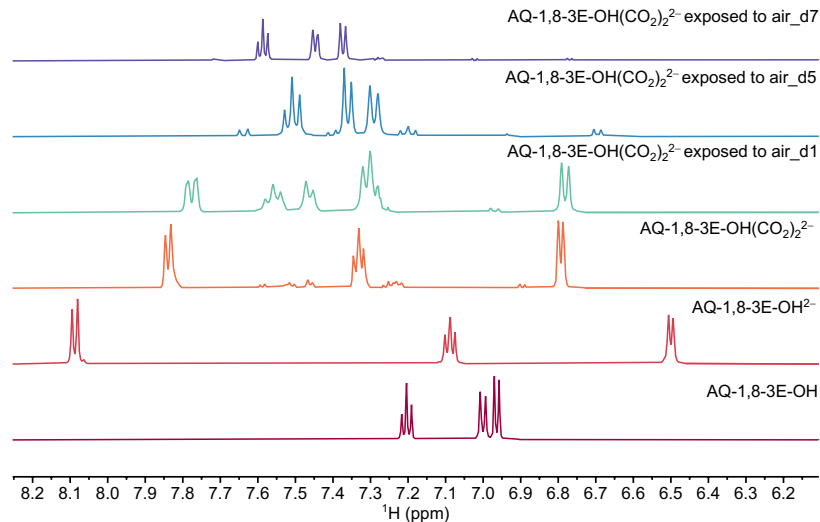


**Figure S19 |  $^1\text{H}$  NMR tracking of chemically synthesized 0.1 M AQ-1,8-3E-OH( $\text{CO}_2$ ) $^{2-}$  in 1 M TBABr D<sub>2</sub>O over days while air was gradually introduced.**

The oxygen sensitivity of 0.1 M AQ-1,8-3E-OH( $\text{CO}_2$ ) $^{2-}$  in 1 M TBABr D<sub>2</sub>O solution was tracked by  $^1\text{H}$  NMR periodically. As shown in the stacked  $^1\text{H}$  NMR spectra, the bottom two are AQ-1,8-3E-OH and AQ-1,8-3E-OH $^{2-}$ , respectivley. The AQ-1,8-3E-OH( $\text{CO}_2$ ) $^{2-}$  was stored in a regular NMR tube and tracked by  $^1\text{H}$  NMR periodically. The regular NMR tube is not air-tight, and air can slowly diffuse to the solution. From day-1 to day-7, the peaks from AQ-1,8-3E-OH( $\text{CO}_2$ ) $^{2-}$  disappeared and instead the peaks of AQ-1,8-3E-OH showed up.

**Table S2 | Coulombic efficiencies of BTMAPAQs | FeNCl flow cells while the BTMAPAQ electrolytes were kept in the atmosphere with different ratios of O<sub>2</sub>/CO<sub>2</sub>/N<sub>2</sub>.** Note that the BTMAPAQ electrolytes were not stirred during the experiments. The anthraquinone electrolytes were just gently flushed by the 1 bar feed gas right above the liquid level.

BTMAPAQ	$\text{O}_2/\text{CO}_2/\text{N}_2$ (%)					
	0/0/100	0/10/90	2.1/10/87.9	5.25/10/84.75	10.5/10/79.5	18.9/10/71.1
1,4-	98.1%	90.3%	58.4%	52.1%	51.7%	44.9%
1,5-	97%	94%	82%	74.5%	60.6%	n/a
1,8-	98%	94%	85%	81%	79%	72%

Given that oxygen can chemically oxidize the reduced anthraquinones, the charge/discharge capacity of anthraquinone electrolytes will become higher/lower than theoretical capacity during charge/discharge processes in the presence of oxygen, thus lowering coulombic efficiencies (CE). Therefore, oxygen sensitivity of the reduced BTMAPAQs can be reflected by coulombic efficiency while varying the ratios of O<sub>2</sub> versus CO<sub>2</sub> in feed gas.

Table S1 lists coulombic efficiencies of 0.1 M 1,4-, 1,5-, 1,8-BTMAPAQ flow cells in the presence of different compositional feed gas. The cells were set to rest for **68 mins** under the feed gas exposure once they were fully charged. The supporting salt used for 1,4-, 1,5-BTMAPAQ is 1 M KCl; the supporting salt used for 1,8-BTMAPAQ is 1 M TBACl. Note that we did not stir the electrolytes to increase the contact area for the gas–liquid phase reactions, as we only aimed to extract the relative oxygen sensitivity trend of the three BTMAPAQs from their CE comparison.

## Chemical CO<sub>2</sub> capture, release, and sequestration procedure in the presence of O<sub>2</sub>

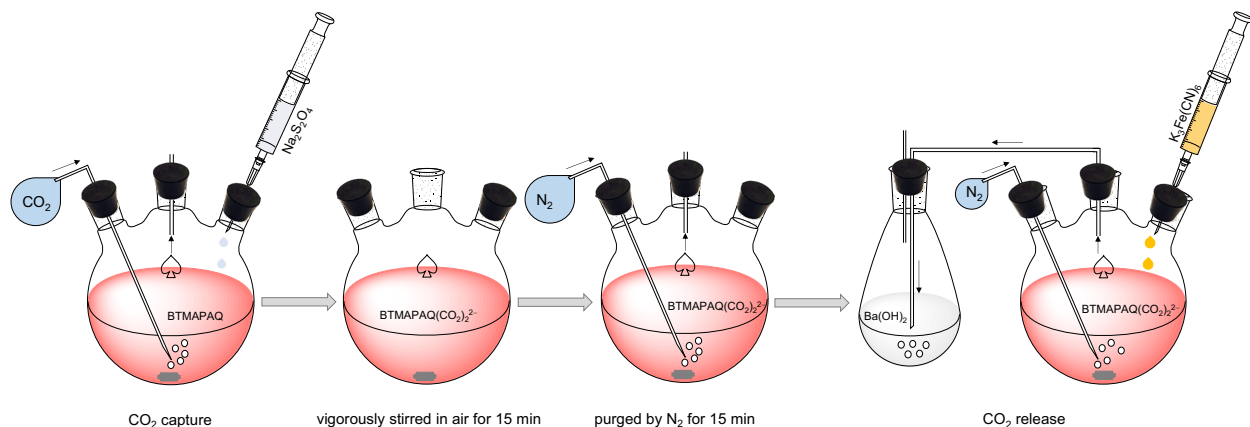


**Figure S20 | Chemically induced CO<sub>2</sub> capture, release, and sequestration.** Capture:  $AQ + S_2O_4^{2-} + 2CO_2 + 2OH^- \rightarrow AQ(CO_2)_2^- + 2HSO_3^-$  (step 1). Release:  $AQ(CO_2)_2^- + 2Fe(CN)_6^{3-} \rightarrow AQ + 2Fe(CN)_6^{4-} + 2CO_2 \uparrow$  (step 2). Sequestration:  $CO_2 + Ba(OH)_2 \rightarrow BaCO_3 \downarrow + H_2O$  (step 3).

Step 1: with continuous CO<sub>2</sub> purging, the flask containing 0.1 M 1,8-BTMAPAQ, 1 M TBACl solution was added with a saturated aqueous solution containing two equivalents of NaOH and one equivalent of Na<sub>2</sub>S<sub>2</sub>O<sub>4</sub>, forming the hemi carbonate [AQ(CO<sub>2</sub>)<sub>2</sub><sup>2-</sup>].

Step 2: the solution was vigorously stirred in air for 15 mins followed with 15-min N<sub>2</sub> purging.

Step 3: with continuous N<sub>2</sub> purging, the flask containing quinone solution was connected with another flask containing saturated Ba(OH)<sub>2</sub> solution prepared in advance under N<sub>2</sub>. With N<sub>2</sub> purging, a saturated aqueous solution containing two equivalents of K<sub>4</sub>Fe(CN)<sub>6</sub> was dropwise added to the quinone solution, generating CO<sub>2</sub> bubbles. The generated CO<sub>2</sub> was carried by N<sub>2</sub> to the Ba(OH)<sub>2</sub> flask, immediately forming cloudy BaCO<sub>3</sub>.

The resulting suspension was centrifuged to collect the precipitates which were then dried in an oven completely until the dry mass becomes constant. The CO<sub>2</sub> capture capacity was calculated from the dry mass of BaCO<sub>3</sub>. The power was cooled down in a desiccant then quickly weighed in a precision balance to obtain the dry mass.

BTMAPAQ chemical reduction/oxidation induced CO<sub>2</sub> capture/release followed with sequestration were designed to determine the carbon capture capacity. We found that 1.7 CO<sub>2</sub> molecules on average were released when the CO<sub>2</sub> chemisorbed solution was stirred in air for 15 mins. 0.3 CO<sub>2</sub> per 1,8-BTMAPAQ was trapped in solution due to oxygen effect (see oxygen-involved side reactions in Table 1).

## Electrochemical CO<sub>2</sub> capture in the presence of O<sub>2</sub>

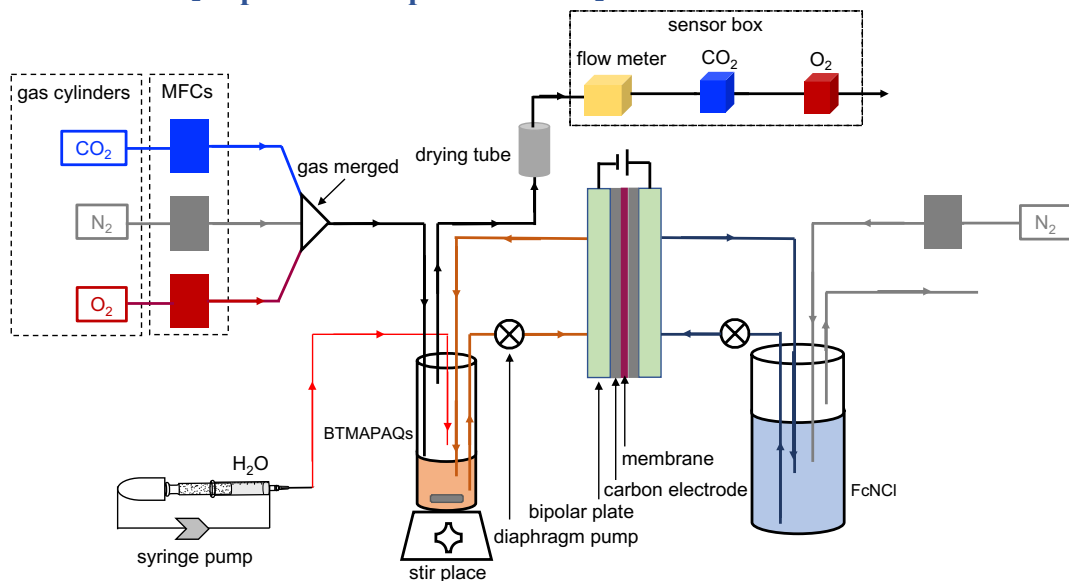


**Figure S21 | Schematic of the electrochemical CO<sub>2</sub> setup in the presence of O<sub>2</sub>.**

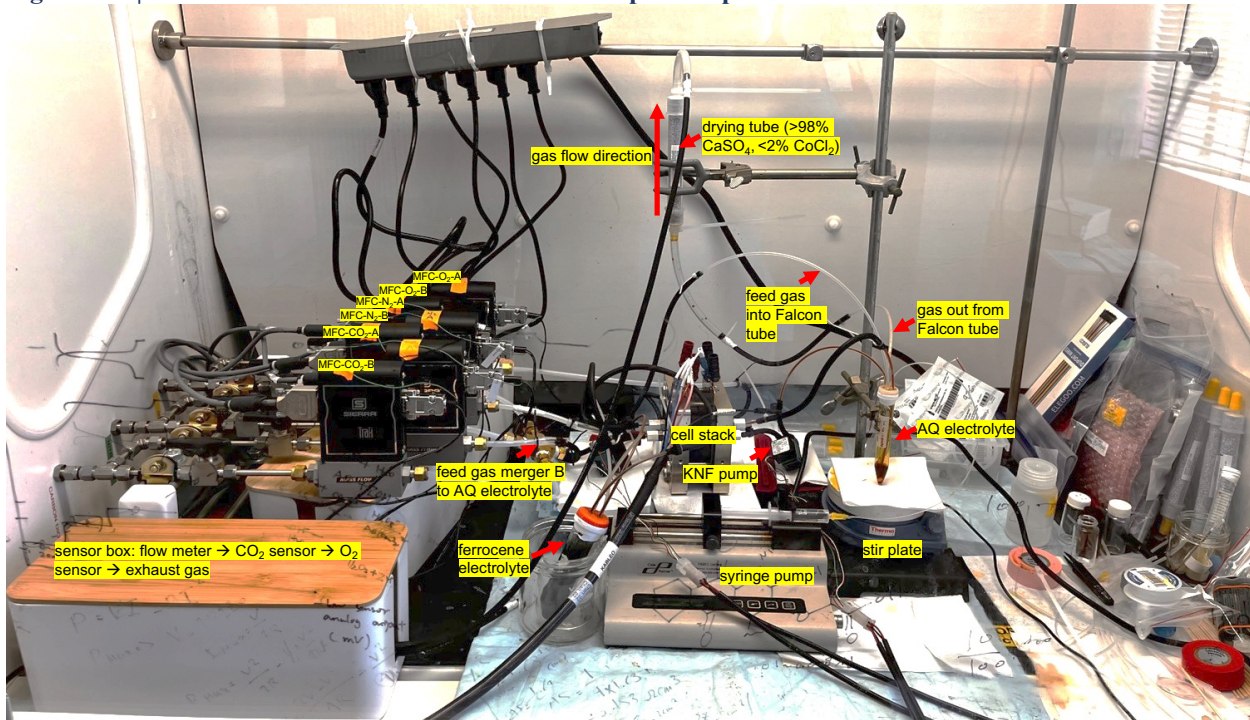


**Figure S22 | Setup of electrochemical CO<sub>2</sub> capture with aqueous quinone flow chemistry.** Mass flow controller (MFC) were controlled by Arduino UNO. MFC-O<sub>2</sub>-A, MFC-N<sub>2</sub>-A, and MFC-CO<sub>2</sub>-A gas tubes were merged and introduced to the ferrocene electrolyte. MFC-O<sub>2</sub>-B, MFC-N<sub>2</sub>-B, and MFC-CO<sub>2</sub>-B gas tubes were merged and introduced to the anthraquinone electrolyte.

FCT flow cell was used for the electrochemical tests. KNF diaphragm pumps were used to circulate electrolytes through the flow fields and electrodes in the cell stack. Unbaked AvCarb HCBA was used as electrodes. DSV-N was selected as the anion-exchange membrane. 15 mL and 50 mL Falcon tubes were chosen as anthraquinone and ferrocene electrolyte reservoirs, respectively.

To avoid humidity interfering sensor detection, before gases flow into the gas sensors which are sitting in the sensor box, a drying tube full with >98% CaSO<sub>4</sub>, <2% CoCl<sub>2</sub> is introduced to the gas line of anthraquinone electrolyte side.

A syringe pump was used to automatically compensate water loss due to the constant gas flow carrying moisture out from the anthraquinone electrolytes.

A football-shape mini stir bar was added into the anthraquinone electrolyte reservoir; under of which, a stir plate was placed to stir the electrolyte during the test to increase the contact area between liquid phase and gas phase.

FS4001 MEMS Mass Flow Sensor, LuminOX O<sub>2</sub> sensor (CM-42990), SprintIR CO<sub>2</sub> sensor (GC-0018) were used in our tests. Biologic SP-150e potentiostat was used as our electrochemical work station.

All of the sensors were calibrated prior to use. Because the partial pressure of the introduced O<sub>2</sub> to the system is only 0.03 bar, 3% of total pressure, 0.15 bar air was introduced and its flow rate was precisely controlled by the mass flow controller.

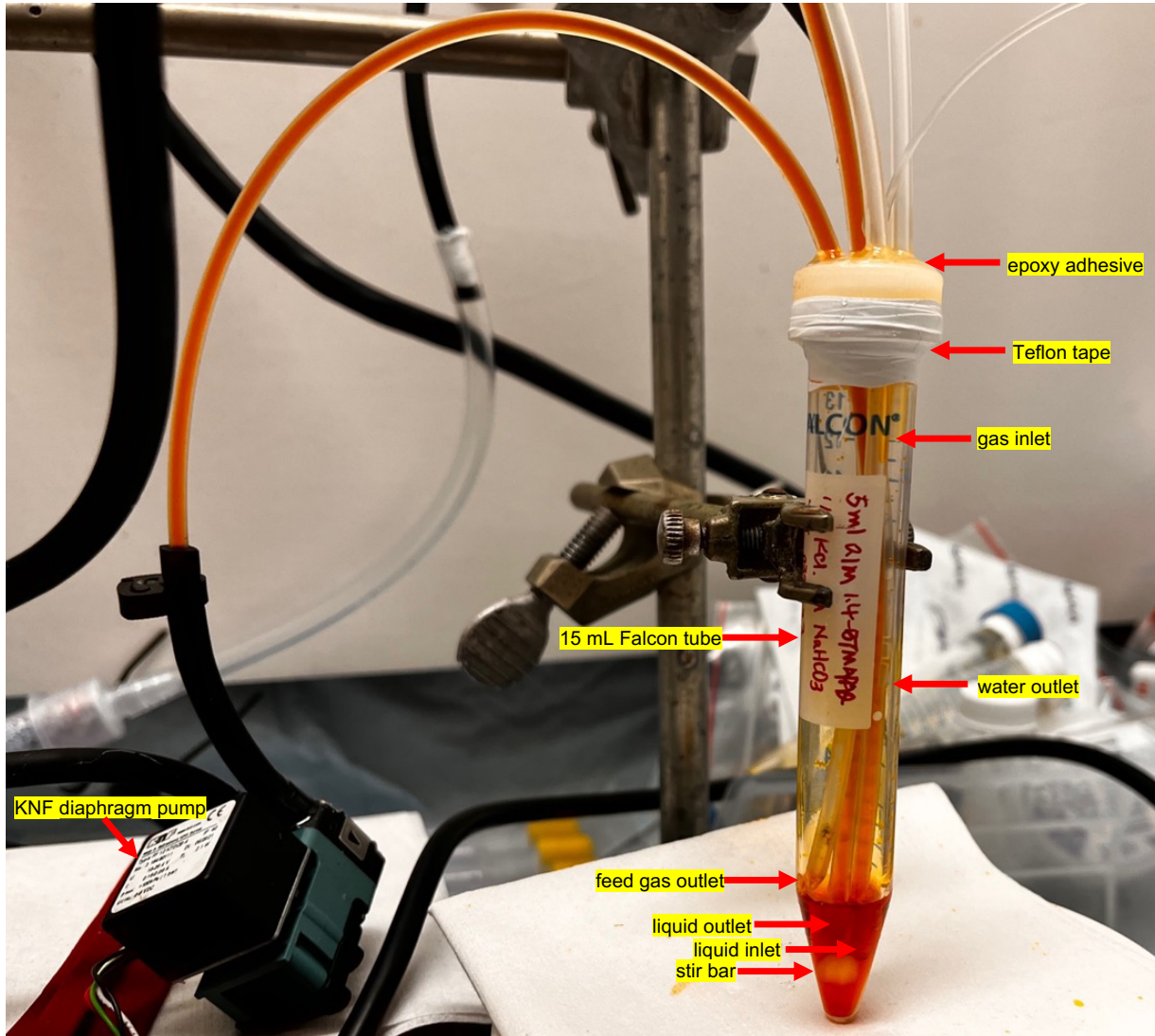


**Figure S23 | A close look of tube positioning in the anthraquinone electrolyte Falcon tube.** Epoxy was used to seal the holes on the cap to avoid any gas leakage. Teflon tape was also used to wrap around the joint of cap and tube body to prevent gas leaking.

The volume capacity of the Falcon tube accommodating the negative electrolytes is 15 mL. 5 mL BTMAPAQ electrolyte was usually prepared as the initial volume. Once being circulated through the cell stack, the remaining volume of BTMAPAQ electrolyte in the Falcon tube is 2 mL, leaving the headspace as 13 mL.

The volume capacity of the Falcon tube accommodating the positive electrolyte is 50 mL. 40 mL FcNCl electrolyte was usually prepared as the initial volume. Once being circulated through the cell stack, the remaining volume of FcNCl electrolyte in the Falcon tube is 37 mL, leaving the headspace as 13 mL.

The liquid flow rate of both positive and negative electrolytes was kept at 70 mL/min. The gas flow rate was kept at ~12 mL/min on both sides. Because of the constant gas purging, we set a syringe pump to automatically compensate the water loss in the negative electrolyte at a rate of 0.01 mL/h.

The viscosity of BTMAPAQ electrolytes is reasonably low and there is no mixing issue. A football shape magnetic stir bar with the dimension of  $\varnothing$  6 mm  $\times$  10 mm was used in the experiments. The stir rate was kept at 800 rpm, that kept whirling the electrolytes, accelerating the gas-liquid reaction.

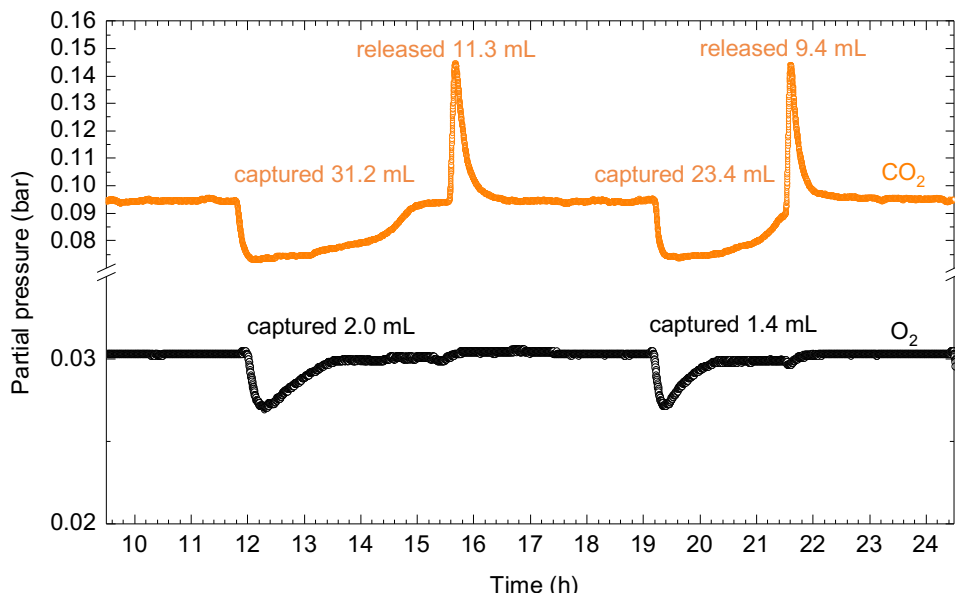


**Figure S24 | Variation of CO<sub>2</sub> and O<sub>2</sub> partial pressure during the electrochemical reduction and oxidation of 1,5-BTMAPAQ electrolyte.** A simulated flue gas composing of 3% O<sub>2</sub>, 10% CO<sub>2</sub>, and 87% N<sub>2</sub> was used as the feed gas stream and constantly introduced to the electrolyte. During and after the electrochemical reudction, the reduced antrahquinone electrolyte became sensitive to O<sub>2</sub> and CO<sub>2</sub>, causing the partial pressure drop for both of them. During the electrochemical oxidation, part of the captured CO<sub>2</sub> by the electrolyte was released, resulting in the CO<sub>2</sub> partial pressure increase. The integrated volumes of released CO<sub>2</sub> are smaller than those of captured CO<sub>2</sub>, because oxygen-involved side reactions can irreversibly trap certain amount of CO<sub>2</sub>, which cannot be released during the normal electrochemical oxidation.

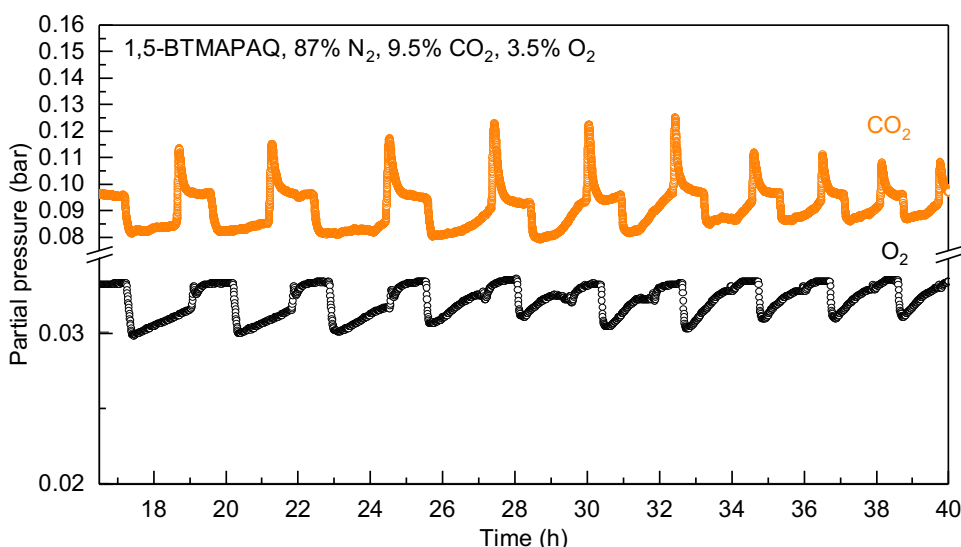


**Figure S25 | Variation of CO<sub>2</sub> and O<sub>2</sub> partial pressure during the electrochemical reduction and oxidation of 1,5-BTMAPAQ in an one bar atmosphere of 87% N<sub>2</sub>, 9.5% CO<sub>2</sub>, and 3.5% O<sub>2</sub>.** Ideally, the O<sub>2</sub> partial pressure drop should align with the CO<sub>2</sub> partial pressure drop because the reduced anthraquinone can simutaneously react with CO<sub>2</sub> and O<sub>2</sub>. The misalignment was caused by the CO<sub>2</sub> meter software artifact.

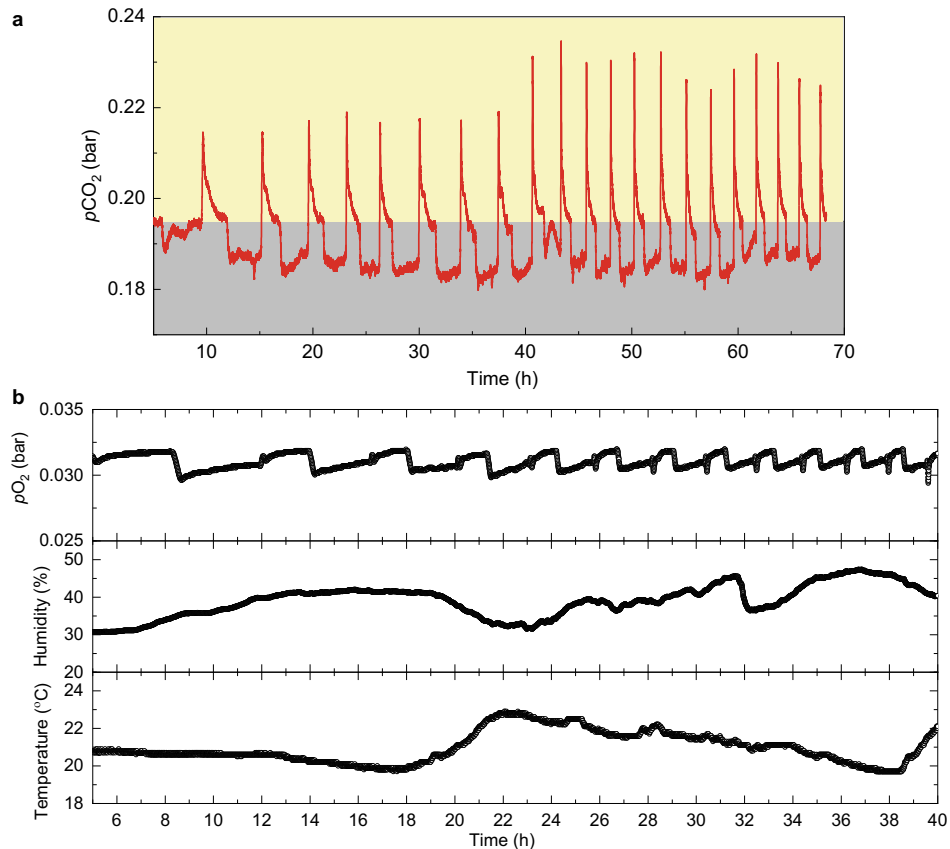


**Figure S26 | Variation of (a) CO<sub>2</sub> and (b) O<sub>2</sub> partial pressure during the electrochemical reduction and oxidation of 1,5-BTMAPAQ in an one bar atmosphere of 77.4% N<sub>2</sub>, 19.5% CO<sub>2</sub>, and 3.1% O<sub>2</sub>. The grey shade highlights the CO<sub>2</sub> capture; and the yellow shade highlights the CO<sub>2</sub> release. (b) Humidity and temperature were also recorded and tracked by the oxygen sensor.**

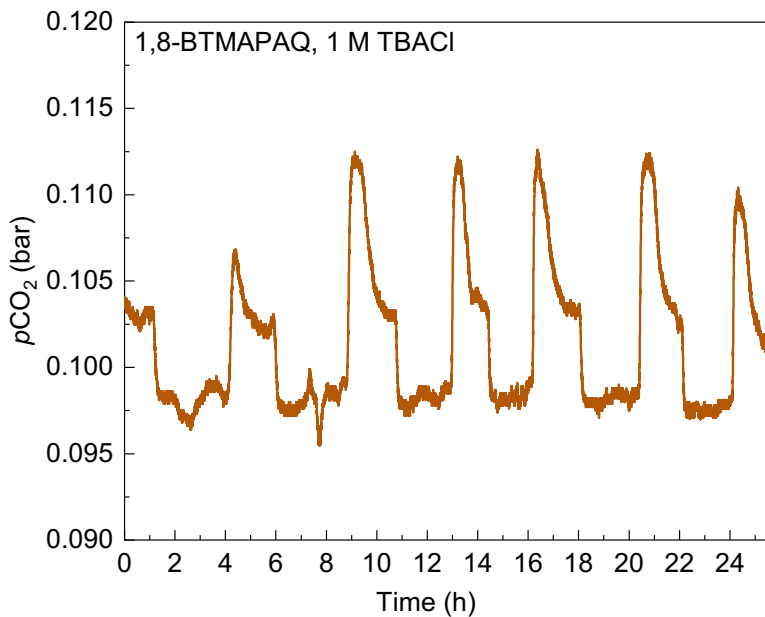


**Figure S27 | Variation of CO<sub>2</sub> partial pressure during the electrochemical reduction and oxidation of 1,8-BTMAPAQ in an one bar atmosphere of 87% N<sub>2</sub>, 10% CO<sub>2</sub>, and 3% O<sub>2</sub>.**

## References:

- <sup>1</sup>Y. Zhu, Y. Li, Y. Qian, L. Zhang, J. Ye, X. Zhang, and Y. Zhao, "Anthraquinone-based anode material for aqueous redox flow batteries operating in nondemanding atmosphere", *Journal of Power Sources* **501**, (2021). <https://doi.org/10.1016/j.jpowsour.2021.229984>
- <sup>2</sup>S. Jin, Y. Jing, D.G. Kwabi, Y. Ji, L. Tong, D. De Porcellinis, M.A. Goulet, D.A. Pollack, R.G. Gordon, and M.J. Aziz, "A water-miscible quinone flow battery with high volumetric capacity and energy density", *ACS Energy Letters* **4**, 1342 (2019). <https://doi.org/10.1021/acsenrgylett.9b00739>
- <sup>3</sup>E.F. Kerr, Z. Tang, T.Y. George, S. Jin, E.M. Fell, K. Amini, Y. Jing, M. Wu, R.G. Gordon, and M.J. Aziz, "High energy density aqueous flow battery utilizing extremely stable, branching-induced high-solubility anthraquinone near neutral pH", *ACS Energy Letters* **8**, 8 (2023). <https://doi.org/https://doi.org/10.1021/acsenrgylett.2c01691>